Universitetet i Stavanger

FACULTY OF SCIENCE AND TECHNOLOGY

MASTER'S THESIS

Study program/specialization: Biological chemistry	Spring semester, 2019 Open
Author: Susanne Nesse	_Susanne Nesse_ (signature of author)
Supervisor(s): Astrid Mork-Jansson (Main supervisor) Jodi Maple Grødem (Co-Supervisor)	
Title of master's thesis: Isolation, characterization and BBB permeability of plasma derived exosomes in relation to refractory epilepsy	
Credits: 60	
Keywords: Biological chemistry, Exosomes, Extracellular vesicles, Drug delivery system, SEC, Exosome characterization, Refractory epilepsy, The blood-brain barrier	Number of pages: 67 + supplemental material/other: 2 Stavanger, 15.06.19 (date/year)

Acknowledgements

I would like to express my appreciation to my supervisor, Astrid Mork-Jansson, for the opportunity to join her exciting research. I am thankful for her guidance and support through the year, and for her patience with my writing and lab work. The thesis could not have been written without her guidance.

Many thanks to Jodi Maple Grødem for her guidance with the confocal microscope and for proofreading my thesis. I would like to thank Julie Nikolaisen for always taking the time to help me in the lab, as well as answering any questions during the year. Thanks to everyone working at CORE, your kind smiles always made my day better.

Finally, I want to thank my family and relatives for all the support, understanding and motivation they gave me.

Abstract

Exosomes have been of increasing interest for researchers due to their potential as a therapeutic drug delivery system. Refractory epilepsy is a drug-resistant form that affects 30% of epilepsy patients. There is no common reason for their resistance, therefore targeted drug therapies may be the best option for improving treatment outcomes. Exosomes are able to cross the blood-brain barrier (BBB) and deliver their cargo still intact to a specific target, making them a promising nanocarrier. At the same time, there exist many challenges in understanding the immune reactions and components of the exosomes.

The lack of an efficient standardized method is a major challenge for utilizing exosomes as a drug delivery system. Size exclusion chromatography (SEC) was tested and optimized to isolate endogenous exosomes from blood plasma. Ultrafiltration was used to purify the samples. The influence of storage conditions on exosomes was tested in order to keep exosomes stable until use. Protein content of vesicle fractions was analyzed by coomassie brilliant blue (CBB) and mass spectrometry (MS). Furthermore, exosomes were characterized by dynamic light scattering (DLS) and western blotting (WB). Exosome uptake in rat astrocytes was studied by confocal microscopy.

It was shown that plasma derived exosomes can be isolated by SEC, and that residual protein was successfully removed by ultrafiltration (100K). Short-term storage of exosomes was confirmed to be best at 4°C or room temperature (20°C). Albumin, immunoglobulin and fibrinogen beta were identified as highly abundant proteins in the vesicle fractions. Fraction 10, 11 and 12 were identified as exosome fractions based on size distribution analysis. Z-average diameter and poly-dispersity (PDI) confirmed fraction 10 and 11 to be exosome fractions with high particle homogeneity. The exosome specific protein, tetraspanin CD9, was identified in fraction 13. Confocal results suggest that exosomes are taken up by rat astrocytes, indicating that exosomes are able to cross the BBB and deliver their cargo.

Abbreviations

Ab	Antibody
ABs	Apoptotic bodies
AEDs	Antiepileptic drugs
BBB	Blood-brain barrier
CBB	Coomassie Brilliant Blue
CD9	Cluster of differentiation 9
CNS	Central Nervous System
DLS	Dynamic Light Scattering
DMEM	Dulbecco´s modified eagle medium
ECL	Enhanced Chemiluminescence
ECM	Extracellular matrix
EVs	Extracellular vesicles
F	Fraction
JAM	Junction adhesion molecules
MS	Mass spectrometry
MVs	Microvesicles
MVBs	Multivesicular bodies
NMKL	Nominal molecular weight limit
NTA	Nanoparticle tracking analysis
PBECs	Porcine brain endothelial cells
PDI	poly-dispersity
SD	Standard deviation
SDS-PAGE	Sodium-Dodecyl-Sulfate Polyacrylamide Gel Electrophoresis
SEC	Size Exclusion Chromatography
TEER	Transendothelial electrical resistance
TEM	Transmission electron microscopy
TJ	Tight junctions
UC	Ultracentrifugation
WB	Western Blot

Table of contents

1. Introduction

1.1 The blood-brain barrier

The blood-brain barrier (BBB) is a highly selective permeability barrier crucial for normal function of the central nervous system (CNS) [1]. The BBB is in general seen as a defense mechanism, regulating and protecting the microenvironment of the brain [2]. The BBB separates the circulating blood from the extracellular fluid in the CNS and regulates the movement of ions and molecules across the barrier [3]. The barrier is formed by capillary endothelial cells which are connected by protein complexes named tight junctions (TJ) and adherens junctions [1]. TJ consist of the integral membrane proteins claudin, occludin and junction adhesion molecules (JAM) in addition to cytoplasmic proteins (Figure 1.1) [4]. When the TJ protein complex binds to the actin-based cytoskeleton it forms a seal, which regulates the permeability and function as a barrier [5]. Adherens junctions consist of a cadherin-catenin complex which links the neighboring cells and regulates cell to cell contact. The transmembrane protein cadherin joins the actin cytoskeleton via catenin proteins and form cell-cell junctions [6].
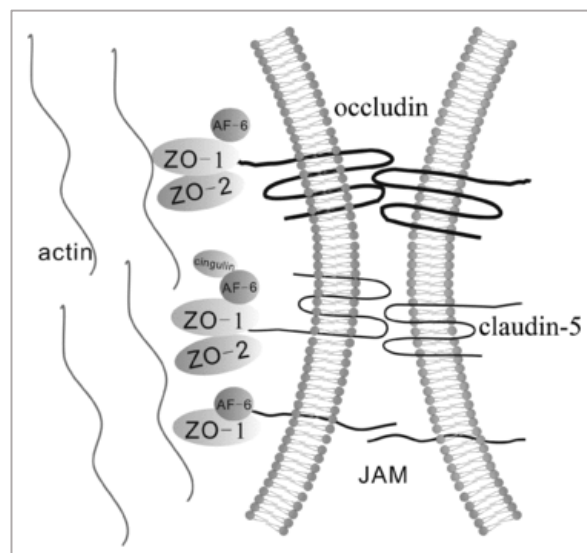

Figure 1.1: Schematic presentation of endothelial TJ in the BBB. The combination of integral proteins (occludin, claudin and JAM) and cytoplasmic proteins (ZO-1, ZO-2, AF-6, cingulin and others) linked to an actin-based cytoskeleton allows the tight junctions to form a seal. Image reprinted under the creative commons license, © 2012 Blackwell Publishing Ltd [4].

Endothelial cell growth and apoptosis are also promoted by junctional proteins through intracellular signals [7]. TJ together with reduced pinocytosis (liquid droplets ingested by cells) and a lack of intracellular fenestrations (gaps which allow water and molecules to pass through) prevent leakage of serum proteins into the CNS [8]. However, molecules are still able to cross the BBB by several mechanisms including facilitated and passive diffusion, extracellular pathways and endocytosis [9].

1.1.1 Drug delivery to the CNS

The BBB is a major obstacle in drug delivery to the CNS due to its regulation of all circulating substances across the barrier [9]. Microvessels cover 95% of the BBB surface area and represent the main pathway for chemicals to enter the brain [10]. Based on our recent understanding of the barrier functions, researchers have developed new strategies for drug transport to the CNS, like delivery through active transporters in the BBB, liposomes, nanoparticles and more [11]. The essential molecules for brain function are transported in through several mechanisms. Only lipid soluble molecules < 400 Da are able to diffuse through the capillary endothelial cells and into the brain [12]. Therefore, liposomes have recently been investigated as nanocarriers to transport drugs across the BBB without damage [10]. Another obstacle in drug delivery is the presence of degrading enzymes inside the endothelial cells, these enzymes recognize and rapidly degrade most peptides crossing the membrane [10]. In addition the BBB has a high concentration of active drug-efflux-transporter proteins (P-glycoprotein), which remove drug molecules before they cross the barrier into the brain [10].

1.1.2 Epilepsy

Epilepsy is a group of neurological diseases characterized by recurrent seizures. An epileptic seizure is defined as abnormal activity in the brain resulting in changed behavior or function [13]. The cause of seizures are in many cases unknown, but genetic factors, brain injury or damage and structural abnormalities during brain development are factors that can lead to epileptic seizures [13]. There are many different types of seizures, and they are categorized into three major groups depending on which part of the brain that is involved [14]. The first group is focal onset seizures where the seizure starts in one side of the brain. Depending on awareness during the seizure it can be subdivided into focal onset aware seizure and focal onset impaired awareness. The second group is called generalized onset seizures, and the

whole brain is involved in this type of seizure. Generalized onset seizures are subdivided into several types, namely tonic clonic, myoclonic, atonic and absence seizures [13]. The last group is called unknown onset seizures, which include seizures with an unknown beginning or seizures that was not witnessed. With more information, the unknown onset seizure may be diagnosed as a focal or generalized seizure [14].

BBB damage or dysfunction can contribute to the development of epilepsy, promote seizures and favor recurrence [15, 16]. Condition changes associated with BBB disruption in epilepsy are down-regulation and loosening of TJ proteins, altered expression of transporter proteins (P-gp, MRP1, MRP2, BCRP) and leakage of albumin, lgG and leukocytes [17]. However, the extent of BBB dysfunction varies [15]. Antiepileptic drugs (AEDs) have the ability to control and protect against seizures while allowing normal function of the nervous system [18]. Around 30% of epileptic patients are affected by a condition called refractory epilepsy, a drug-resistant form [19]. Changed BBB morphology, leaky vessels and abnormal neurovascular structure are some of the conditions observed in this form of epilepsy [15]. Patients with refractory epilepsy do not share a common reason for their resistance, therefore targeted drug therapies may be the best option for improving treatment outcomes [20].

1.2 Exosomes

Cells can use extracellular vesicles (EVs) as signaling organelles in long distance intercellular communication [21]. EVs are a general term for all small secreted vesicles, and they are mainly classified as exosomes, apoptotic bodies (ABs) and microvesicles (MVs) [22]. Exosomes are nanovesicles with the size of 50-100 nm [23]. They are generated inside multivesicular endosomes/bodies (MVBs) that are formed by inward budding of the plasma membrane (Figure 1.2). The inward budding results in an equal orientation of protein and lipids as the plasma membrane, but some proteins are exhausted, making the exosomes composition distinct from the plasma membranes [23]. MVBs can either fuse with the plasma membrane, or with a lysosome that leads to digestion of the cargo (Figure 1.2). When the MVBs fuse with the plasma membrane it results in release of exosomes [23]. Exosomes are frequently released as small aggregates, and they can transfer their cargo to recipient cells [24]. The exosomes and target cells interact through target cell dependent reactions, like receptor binding, fusion to the target cell, and internalization by endocytosis [23]. The exact biological functions of exosomes are still to be unraveled. However, there is evidence that the

exosomes play an important role in many cellular processes, like intercellular communication, immune reactions, waste handling and transfer of nucleic acids and proteins [23, 25].
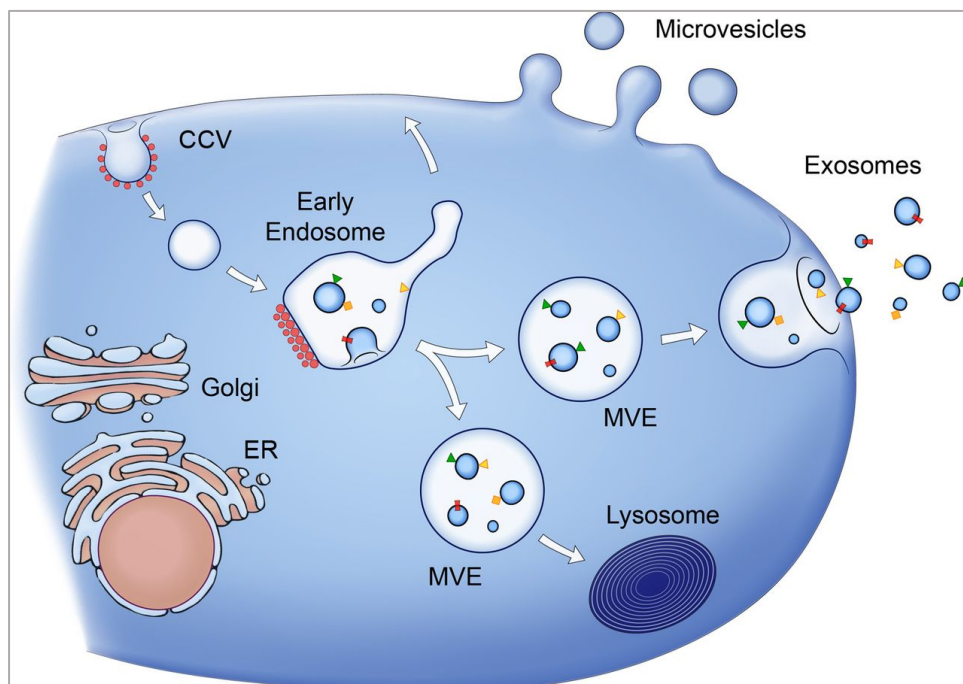
Figure 1.2: Formation and release of exosomes. Inward budding of the plasma membrane forms MVB (MVE), which generates exosomes inside. MVBs have two pathways; either fuse with the plasma membrane to release exosomes, or fuse with a lysosome to digest the cargo. Since the plasma membrane buds inwards the receptors on the surface of the plasma membrane is located inside the MVBs, these membrane-associated proteins are represented as rectangles and triangles. Image reprinted under the creative commons license, © 2013 Raposo and Stoorvogel [26].

Exosomes contain a selection of different biologically active molecules including proteins, miRNAs and mRNAs, that regulate cellular function and gene expression in the target cell [21]. The fact that they are able to deliver their cargo still intact, to a specific target over a long distance makes them a promising drug delivery system [23]. The major advantage of exosomes compared to other synthetic nanoparticles, is that self-derived exosomes will not provoke an immune response in the human body, consequently leading to a long and stable circulation in the blood [11]. Exosomes are similar to liposomes in having a bilayer lipid membrane and an aqueous core, making them able to carry both hydrophilic and lipophilic drugs across the BBB [27]. Because of their small size these vesicles can avoid degradation by macrophages and circulate for a long time within the body [28]. Another advantage of exosomes as a drug delivery system is that there is no unwanted accumulation of exosomes in

the liver [28]. On the other hand, the role of exosomes in health and disease is not fully understood making it complicated to predict a long-term safety and therapeutic effect. Exosomes involvement in tumor growth and enhanced tumor cell survival is also a huge concern [28]. There exist many challenges in understanding the immune reactions and components of the exosomes before they can be used as a drug delivery system.

1.2.1 Exosomes in the Central Nervous System

Most cell types in the CNS, including neurons, astrocytes, glial cells and oligodendrocytes are believed to secrete exosomes [29]. Studies reveal that exosomes in the CNS are linked to many different processes, such as communication, neural development, protective mechanisms and synaptic activity [29, 30]. Astrocytes are important in defense, development and homeostasis of the CNS, and are observed to release exosomes as a response to stress and also in pathological conditions [31]. Given that exosomes can cross the BBB in both directions and transfer their cargo without cell-to-cell contact, researchers are considering exosomes as a potential nanocarrier to transport drug molecules into the brain [29]. In order to use exosomes as a delivery system it is crucial to know the specific functions and their biological roles in the CNS. The fact that endothelial cells and astrocytes release their own exosomes can complicate the analysis of exosome uptake in cell lines. Neural secreted exosomes carry protein markers inherited from their cellular origin, namely cell adhesion molecule L1, GPI- anchored prion protein and glutamate receptors [32]. This feature may be utilized to distinguish neural exosomes from applied exosomes in the analysis.

1.2.2 Exosome isolation

Even though exosomes were discovered more than three decades ago [33], these small EVs have been of increasing interest for researchers due to their potential as a therapeutic delivery system [34]. Exosomes are observed in most viable cells, and are present in all biological fluids of the body, like blood, lymph liquid, urine and more [35]. In order to study the exosomes, it is crucial that they are isolated from all interfering components. Isolation of plasma derived exosomes is difficult due to the high viscosity of blood and the presence of many proteins and lipoproteins, including fibrinogen and albumin [36, 37]. In addition they are derived from many different cell types, like endothelial cells, leukocytes, platelets and red cells, which again complicates their analysis [38]. Many different exosome isolation techniques are developed, and each technique uses a specific characteristic of exosomes to aid

the isolation. Still there is no efficient method for isolation of exosomes from biological fluids without impurities [39]. Each protocol needs to be optimized depending on the source of biological sample in order to achieve a high yield of exosomes without impurities, and often several methods are combined.

Ultracentrifugation (UC) is one of the most commonly used isolation methods. In this method a centrifugal force is applied to selectively sediment the components according to their size, density and mass. A schematic workflow of the isolation method is presented in Figure 1.3. For plasma samples a cleaning step is often applied prior to isolation in order to remove large particles and to add protease inhibitors to prevent degradation of exosomal proteins [25]. UC is easy to use, requires little sample pretreatment and is affordable over time. At the same time this method is time consuming, and often suffers from contamination and exosome loss due to the overlap in size of the extracellular vesicles [25]. Previous studies show that only a minority of exosomes are isolated from blood plasma by this method [39].
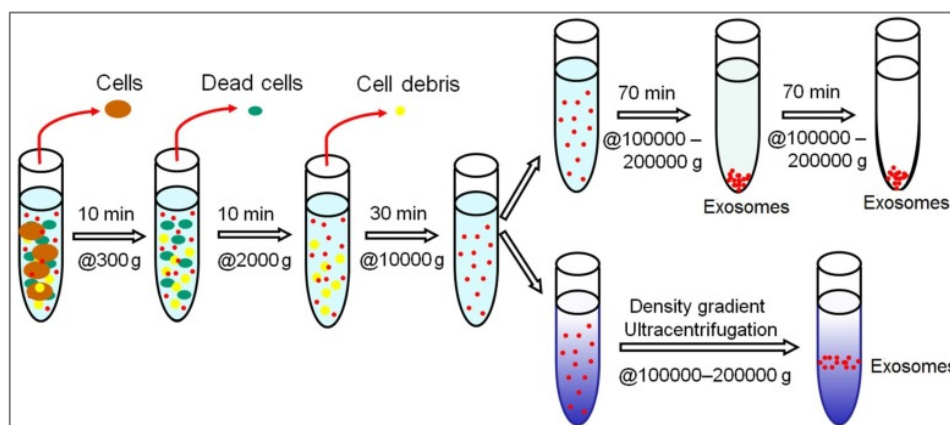
Figure 1.3: Workflow of exosome isolation by UC. Differential ultracentrifugation leads to a pellet of exosomes, while density gradient ultracentrifugation separates the exosomes as a layer based on their density. Image reprinted under the creative commons license, © Ivyspring International Publisher [25].

Size exclusion chromatography (SEC) separates molecules in a solution based on size, thus separating the exosomes from other EVs. The principle of isolation by SEC is shown in Figure 1.4. This method is proposed to isolate exosomes from blood plasma without significant impurities [40] and has a lower albumin contamination compared to UC [39]. SEC maintains the vesicular structure and conformation of the exosomes and has a short sample processing time. However, it requires time for preparation and washing of the column. The

manual collection of fractions may introduce variability and can affect the purity [41].
Another limitation is the dilution of the samples, which may require an additional
concentrating step that can lead to yield loss.
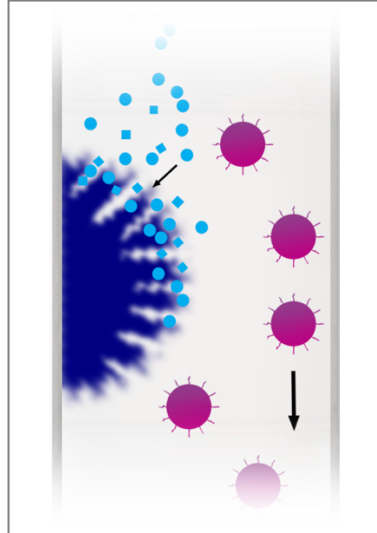
Figure 1.4: The principle of isolation by the qEV SEC column. The column uses a stationary
phase of porous resin particles, where smaller molecules will enter and be slowed down.
Larger molecules will flow around the resin and are eluted from the column earlier. Image
reprinted under the creative commons license, © IZON SCIENCE LTD 2018.

Another exosome isolation method is immunoaffinity capture, this method utilizes antibody
coated magnetic beads to capture exosomes with a specific antigen [42]. This allows
exosomes to be isolated based on their origin or subpopulation. Immunoaffinity capture can
also be used in addition to other isolation methods to achieve more purified exosomes [25].
Exosomes isolated by immunoaffinity capture have a higher purity than others, but at the
same time lower yields are obtained. There is also a possibility that the coated beads can be
masked or blocked [25]. Still, despite the low yield, this method is ideal if one wishes to
isolate a specific subpopulation of exosomes.

1.2.3 Detection and characterization of exosomes

Known features, such as size, molecular composition, morphology and concentration are
utilized for characterization of exosomes. However, the small size of EVs presents a
significant challenge in quantitative analysis. Exosomes from plasma are derived from many
different cell types which complicates their analysis. Various optical and non-optical methods

have been developed for the assessment of EVs, however optimization and standardization of the methods remains an important task. A standardized method for characterization of exosomes is required in order to explore their possibilities as a drug delivery system. Several methods can be used for characterization, like nanoparticle tracking analysis (NTA), transmission electron microscopy (TEM) and western blotting (WB) [43]. However multiple techniques are often required to get the best characterization of exosomes [44].

NTA is a technique where a laser light scattering microscope is combined with a camera to enable the visualization and recording of nanoparticles in a liquid suspension. The method relates the rate of Brownian motion to particle size, and gives information about size, particle distribution and relative concentration of microvesicles in the suspension [37]. Exosomes can be difficult to distinguish from other membrane microvesicles in NTA, however incorporation of fluorescently coupled antibodies might allow the detection of a specific microvesicle [45]. Detection of exosomes derived from cell lines require a serum-free medium to reduce the background signal, not all cells tolerate these conditions which may further influence the results [45]. At the same time this technique provides information about how many microvesicles that are present in a sample, leading to a better standardization of systems.

TEM is a characterization method that uses electrons to create a high resolution image of nanoparticles to determine their size and morphology [37]. The sample preparation is complicated and previous studies report that TEM detect fewer particles compared to NTA [46]. The extensive preparation, including fixing and dehydration, can easily result in changed morphology of exosomes [43]. In addition, there is a possibility that the electron beam can cause damage to biological samples.

Characterization of exosomal protein is often conducted by WB. Tetraspanin proteins are exosomes-associated surface markers resulting from exosome formation in MVBs used as markers to identify exosomes [23]. Tetraspanins (CD9, CD63, CD81 and CD82) are proteins composed of four transmembrane proteins and are not found in other types of vesicles of similar size [26]. Other protein markers include heat shock protein 70 (HSP70), tumor susceptibility gene 101 (TSG101), flotillin 1 and ALG-2 interacting protein X (ALIX) [28]. WB on its own cannot identify exosomes, but is often used as an additional method to confirm exosomal proteins present in purified EV preparations [47].

1.3 Objectives

Objectives of this thesis were to:

- isolate and characterize endogenous exosomes,
- study the BBB permeability of endogenous exosomes in the BBB hCMEC/D3 cell line, and
- investigate exosome uptake in rat astrocytes.

Refractory epilepsy is a drug-resistant form that affects 30% of epilepsy patients. Although there are many new AEDs available, this has had little effect on the resistant patients. There is no common reason for their resistance, therefore targeted drug therapies may be the best option for improving treatment outcomes. The BBB is a highly selective permeability barrier and a great hurdle for drug delivery into the brain. To investigate exosomes as a drug delivery system in neurological diseases, it is important to verify that exosomes are able to cross the BBB to deliver their cargo. A major advantage of exosomes compared to other synthetic nanoparticles, is that self-derived exosomes will not provoke an immune response in the human body, consequently leading to a long and stable circulation in the blood. Lack of an efficient standardized isolation method is a major challenge for utilizing exosomes as a drug delivery system. Isolation of plasma derived exosomes is difficult due to the high presence of proteins, and it is crucial that they are isolated from all interfering components.

In order to address these challenges, SEC was tested and optimized as an isolation method for endogenous exosomes from plasma. Characterization methods were applied to confirm the size, homogeneity and composition of the isolates. Furthermore, as exosomes have a potential ability to cross the BBB, the BBB hCMEC/D3 cell line was exposed of endogenous exosomes to study the BBB permeability. Astrocytes are the most abundant type of glia cell in the CNS, and rat astrocytes from Denmark were used to investigate exosome uptake. The astrocytes were incubated with exosomes followed by visualization in a confocal microscopy to verify exosome uptake. This project, as a part of the larger exosome study, will aid in the investigation of a better exosome isolation from plasma, as well as investigating the BBB permeability of endogenous exosomes and exosome uptake in rat astrocytes.

2. Materials

2.1 General reagents

Material/Chemical	Supplier	Catalog Number	Unit Size
Acetonitrile	Thermo Scientific	89871C	24 mL
Ethanol 95%	Solveco	64-17-5	1 L
HCl	Sigma	H1758	500 mL
Hydrogen peroxide 30% stabilised	VWR Chemicals	23619.297	1 L
Methanol	VWR Chemicals	83809	5 L
Nonidet P-40 Substitute, Proteomics Grade (NP-40)	Amresco	97064-922	50 mL
Potassium chloride	ROTH	6781.3	500 g
Potassium dihydrogen phosphate (KH_2PO_4)	ROTH	3904.1	1 kg
SDS	MERCK	151-21-3	1 kg
Skim milk powder	VWR Chemicals	84615.0500	500 g
Sodium chloride	VWR Chemicals	7647-15-5	1 kg
Sodium deoxycholate	Sigma	D-6750	10 g
Sodium Phosphate (Na_2HPO_4)	G-Biosciences	RC-095	500 g
Trifluoroacetic acid (TFA)	Sigma	T6508	100 mL
Tris-(hydroxymethyl) aminomethane	VWR Chemicals	28811.295	1 kg
Water, Sterile, Nuclease-Free	VWR	97062-790	100 mL

2.2 Isolation of exosomes

Name	Description/supplier
10X PBS 80 g/L NaCl 2.0 g/L KCl 14.4 g/L Na_2HPO_4 2.4 g/L KH_2PO_4	Elution buffer, adjust pH to 7.4

0.5 M NaOH	Column cleanup
20 g NaOH	
1000 mL distilled water	
Amicon Ultra-0.5 mL Centrifugal Filters (3K and 100K device)	Merck
Blood plasma	From donor with epilepsy
qEVoriginal Size Exclusion Columns	iZON Science

2.3 SDS PAGE

Name	Description/supplier	Catalog Number
10X Bolt™ Sample Reducing Agent	Invitrogen	B0009
20X Bolt™ MES SDS Running Buffer	Invitrogen	B0002
4X Bolt™ LDS Sample Buffer	Invitrogen	B0007
Bolt™ 10% Bis-Tris Plus Gels, 1.0mm 12-well	Thermo Scientific	NW00102BOX
Mini Gel Tank	Thermo Scientific	A25977
Seeblue™ Plus2 Prestained Standard	Invitrogen	LC5925

2.4 Solutions Coomassie Blue Staining

Name	Description
Coomassie Blue	
0.1 % Coomassie Brilliant Blue	
50% Methanol	
10 % Glacial acetic acid	
Destaining	
40% Methanol	
10% Glacial acetic acid	

2.5 Immunoblotting

Name	Description/supplier
10X Transfer buffer (1000 mL)	pH 8.3 (do not need to adjust pH)
30.3 g Tris	
144 g Glycine	
Distilled water to 1000 mL	
1X Transfer buffer	Gel to membrane transfer
5 mL Methanol	
45 mL 1X transfer buffer	
1M Tris-HCl (pH 7.5)	
12.11 g Tris	
80 mL distilled water	
Adjust pH to 7.5 with HCl	
Distilled water to 100 mL	
5M NaCl (500 mL)	
146.1 g NaCl	
Distilled water to 500 mL	
1X TBS (1000 mL)	Dilution of Ab and wash of membrane
10 mL 1M Tris-HCl (pH 7.5)	
30 mL 5M NaCl	
Distilled water to 1000 mL	
5% Blocking buffer	Blocking of membrane
150 mL 1X TBS	
7.5 g non-fat dry milk	
1Ab dilution (1:1 000)	CD9 rabbit-anti-human, ExoAb
10 mL 5% blocking buffer	Antibody Kit, EXOAB-KIT-1, System
10 µL primary antibody	Biosciences

2Ab dilution (1:20 000)

20 mL 5% blocking buffer

1 μL goat anti-rabbit HRP secondary antibody

Goat anti-rabbit HRP secondary antibody, ExoAb Antibody Kit, EXOAB-KIT-1, System Biosciences

2M Tris-HCl (pH 8.3)

24.22 g Tris

80 mL distilled water

Adjust pH to 8.3 with HCl

Distilled water to 100 mL

ECL 1 (10 mL)

500 μL 2M Tris-HCl (pH 8.3)

100 μL luminol

100 μL p-coumaracid

9.3 mL distilled water

Light sensitive, cover with aluminum

ECL 2 (10 mL)

500 μL 2M Tris-HCl (pH 8.3)

6.1 μL H_2O_2

9.5 mL distilled water

Amersham™ Protran® Premium Western blotting membranes, nitrocellulose	GE Healthcare Life Sciences
ChemiDoc Touch Imaging System	Bio-Rad
Grade 3MM Chr Blotting Paper, sheet, 46 × 57 cm	GE Healthcare Life Sciences
Image Lab version 5.2.1	Bio-Rad
Pierce G2 Fast Blotter	Thermo Scientific

2.6 Solutions In-Gel Tryptic Digestion

Name	Description
Destaining solution 80 mg ammonium bicarbonate 20 mL acetonitrile (ACN) 20 mL ultrapure water	May be stored at 4°C for 2 months
Reducing buffer (one sample) 3.3 µL TCEP 30 µL digestion buffer	Prepare just before use
Alkylation buffer 5X stock solution: 7 mg iodoacetamide (IAA) 70 µL ultrapure water Final Alkylation buffer (one sample): 7 µL of 5X stock solution 28 µL digestion buffer	Prepare just before use, in a brown tube to avoid light exposure
Digestion buffer 10 mg ammonium bicarbonate 5 mL ultrapure water	May be stored at 4°C for 2 months
Trypsin working solution Dilute Trypsin Stock 10-fold by adding 45 µL of ultrapure water	Can be stored at -20°C for 2 months without activity loss
Activated trypsin 1 µL trypsin working solution 9 µL digestion buffer	Prepare shortly before use, and store on ice until use

2.7 Pierce C18 Spin Columns

Name	Description/supplier
Activation solution 50% methanol (ACN can be substituted for methanol)	400 µL needed per sample
Equilibration solution 0.5% TFA 5% ACN	400 µL needed per sample
Sample buffer 2% TFA 20% ACN	1 µL sample buffer needed for every 3 µL sample
Wash solution 0.5% TFA 5% ACN	400 µL needed per sample
Elution buffer 70% ACN	40 µL needed per sample
Pierce™ C18 Spin Columns	Thermo Scientific

2.8 Exosome Lysis

Name	Description
5X RIPA buffer (50 mL) 6.25 mL 1M Tris-HCl pH 7.6 2.19 g NaCl 2.5 mL NP-40 1.25 g Sodium deoxycholate 0.25 g SDS	

Digital Sonifier		Branson

2.9 Cell Culture BBB hCMEC/D3

Name	Catalog Number	Supplier
PBS Tablets	18912014	Life Technologies
75 cm Tissue Culture Flask, 250 mL, Vented Cap	353136	Falcon
Blood-Brain Barrier hCMEC/D3 Cell Line	SCC066	Millipore
Collagen I, Rat tail, 3mg/mL	A1048301	Gibco
Dimethyl Sulfoxide for cell culture (DMSO)	A3672	Applichem
Fibroblast growth factor 2 (FGF-2)	GF003	Sigma
Low temperature freezer vials, 2mL	479-1262	VWR
Microtube, 1.5mL	16466-030	VWR
Mr. Frosty™ Freezing Container	15-350-50	Thermo Scientific
Muse™ Cell Analyzer		Millipore
Muse™ Count & Viability Reagent	MCH600103	Millipore
Penicillin-Streptomycin, liquid	15140122	Life Technologies
Tissue Culture Plates, 6 wells, sterile	734-2323	VWR
Trypsin-EDTA solution	T4049	Sigma

2.10 Isolation of Primary Porcine Endothelial Cells

Name	Catalog Number	Supplier
Complete culture medium		
450 mL DMEM		
50 mL FBS		
5 mL Pen-strep		
Freezing medium		
90% DMEM complete culture medium		
10% DMSO		
Collagenase type II	17101015	Life Technologies
Dimethyl Sulfoxide for cell culture (DMSO)	A3672	Applichem

Dulbecco´s modified eagle´s medium (DMEM) low glucose (With glucose and sodium bicarbonate, without L-glutamine)	D5546	Sigma
DNase I	18047019	Life Technologies
FBS fetal bovine serum	S1860	Biowest SAS
PBS Tablets	18912014	Life Technologies
Penicillin-Streptomycin, liquid	15140122	Life Technologies
Pig Brains		From slaughterhouse
Trypsin-EDTA solution	T4049	Sigma

2.11 Cell Culture - Astrocytes

Name	Catalog Number	Supplier
PBS Tablets	18912014	Life Technologies
Calf Serum (Heat inactivated)	S040H-500	Biowest
Penicillin-Streptomycin, liquid	15140122	Life Technologies
Poly-L-Lysine	AR0003	Boster
Rat astrocytes		From Denmark
Trypsin-EDTA solution	T4049	Sigma

2.12 Confocal microscopy

Name	Catalog Number	Supplier	Description
PBEC Assay Hanks balanced salt solution (HBSS) 25mM HEPES 0.5% BSA			Used to dilute exosomes
10X PBS+ (with calcium and magnesium) 80 g/L NaCl 2.0 g/L KCl 14.4 g/L Na_2HPO_4 2.4 g/L KH_2PO_4			Adjust pH to 7.4 Used to wash stained exosomes

1.1 g/L CaCl$_2$			
0.5 g/L MgCl$_2$			
Immersion oil	-	Nikon	
Microscope slides	-	VWR	
VECTASHIELD Antifade Mounting Medium with DAPI	H-1200	Vector laboratories	
Wheat Germ Agglutinin (CF®488A)	29022-1	Biotium	Ex 490/ Em 515
Wheat Germ Agglutinin (CF®640R)	29026-1	Biotium	Ex 642/ Em 662
Hank´s BSS (1x)	H15-009	Thermo Scientific	

2.13 Kits

Name	Catalog Number	Supplier
EndoGRO^{TM} MV Complete Culture Media Kit	SCME004	Millipore
ExoAb Antibody Kit (CD9, CD63, CD81, Hsp70 antibodies, rabbit anti-human) with goat anti-rabbit HRP secondary antibody	EXOAB-KIT-1	System Biosciences
In-Gel Tryptic Digestion Kit	89871	Thermo Scientific
Muse^{TM} Count & Viability Kit	MCH600103	Millipore
Pierce BCA Protein Assay Kit	23227	Thermo Scientific

3. Methods

3.1 Experimental strategy

This study covered the isolation of endogenous exosomes from blood plasma, followed by characterization by DLS, CBB, WB and MS. The BBB hCMEC/D3 cell line was exposed to endogenous exosomes to determine BBB permeability by MS. Porcine brain endothelial cells were isolated for future exosome uptake studies. Furthermore, rat astrocytes were grown and exposed to exosomes in order to study exosome uptake in a confocal microscope.

3.2 Isolation of endogenous exosomes by SEC

Exosomes originating from blood plasma were isolated by Size Exclusion Chromatography (SEC) with the use of a qEVoriginal SEC column. Here, the EVs are separated by size while maintaining their biological properties. The column uses a stationary phase of porous resin particles, where smaller molecules will enter and be slowed down. Larger molecules will flow around the resin and are eluted from the column earlier. By the use of phosphate-buffered saline (PBS) EVs are isolated and collected in different fractions (F). The qEV SEC column is proven to give a good recovery of vesicles with removal of background proteins and other contaminants [36].

Blood plasma from a donor was centrifuged twice for 15 min, 2500xg and 4°C to eliminate other cellular components. The platelet free plasma (supernatant) was separated by SEC. Before separation the SEC column was rinsed with 10 mL degassed 1X PBS to avoid air bubbles forming in the gel bed. The column was leveled and equilibrated to room temperature, buffer above the top filter was removed and 500μL sample was applied to the column. The larger vesicles; apoptotic bodies and micro-vesicles, were eluted in degassed 1X PBS in the first 3 mL (F1-F6), followed by the vesicle fractions where exosomes were expected to elute (F7-F13). After elution of sample the column was washed with 10 mL degassed 1X PBS and stored in 20% ethanol (degassed).

3.3 Dynamic light scattering

Dynamic light scattering (DLS) was used to analyze vesicle fractions F7-F13 to determine the size and homogeneity of vesicles eluted. DLS is a non-invasive technique used to determine particle size based on the relationship between light scattering and diffusion behavior of particles [48]. The cuvette was washed with 70% ethanol followed by distilled water, all the remaining water was pipetted out to not dilute the samples. Dust particles may affect the DLS measurements as they scatter light, therefor it is important to ensure sufficient cleaning [48]. 50μL of each fraction was pipetted into the cuvette and the size was measured at 25°C by Zetasizer Nano ZSP (Malvern, UK) and Zetasizer software. The size distribution results from Zetasizer were transferred to excel where a plot between size (d.nm) and intensity (%) was made. The quality result of each sample was also controlled to be of good quality. The size distribution by intensity is based on the assumption that the correlation function consists of a sum of different contributions from different particle sizes. Z-average diameter and poly-dispersity (PDI) values of the fractions were also retrieved from the software. Where z-average is an intensity based mean diameter derived from the cumulants analysis, and PDI an indicator of the width of the overall distribution assuming a single mean.

3.4 Ultrafiltration of vesicle fractions

The vesicle fractions were ultrafiltrated to remove residual proteins and to concentrate the vesicle fractions. Amicon Ultra 0.5 mL Centrifugal Filters were used to filtrate the samples, and the method was conducted as stated in the user guide [49].

500 μL sample was added to the 100K filter device and centrifuged for 5 min, 14 000xg at RT, resulting in a 9-fold up-concentration. To recover the concentrated solute, the filter was placed upside down in a new centrifugal tube and centrifuged for 2 min, 1000xg at room temperature. Both the 3K and 100K filter devices were tested for best removal of macromolecular components. The filter devices are characterized by a nominal molecular weight limit (NMWL), which means they retain molecules above a specified molecular weight [49]. The 3K device has a 3,000 NMWL and the 100K device has 100,000 NMWL.

3.5 Exosome lysis

Exosomes were lysed and compared to non-lysed samples on CBB and WB. 2X RIPA buffer was added 1:1 to the sample, followed by 10 seconds sonication and incubation for 15 min at 4°C. The RIPA buffer enables protein solubilization and extraction of proteins from the membrane.

3.6 Protein and lipid quantification

The total protein concentration can give an indicator on the recovery after isolation and can be used as an approximation of protein removal after ultrafiltration. Total protein content was also determined in order to load equal amount of protein in SDS-PAGE. Absorbance was applied to compare protein contamination (280 nm) and lipid (498 nm) content in the different fractions during storage.

3.6.1 BCA Protein Assay

The total protein concentration of the vesicle fractions was estimated by using the Pierce BCA Protein Assay Kit. Diluted albumin (BSA) standards and working reagent were prepared as stated in the kit protocol [50]. The microplate procedure was followed by pipetting 25 μL of each standard or sample, and 200 μL working reagent to each well. The plate was covered by aluminum and incubated for 30 minutes at 37°C. After incubation the plate was cooled down to room temperature and absorbance was measured at 562 nm by the SpectraMax spectrophotometer. Results were retrieved by SoftMax pro 6.2.1 software.

3.6.2 A280, protein absorption

An evaluation of ultrafiltration as a possible method for protein removal was performed by determining protein quantification before and after ultrafiltration by NanoDrop One (Thermo Scientific). 2 μL sample was loaded and protein method "Protein A280" was selected.

3.6.3 Absorbance reading of protein and lipid content

For further analyzation of protein contamination and lipid content, absorbance of the different fractions was measured at 280 nm (protein) and 498 nm (lipid). 50 μL of each sample was

added to a microplate and absorbance was measured by the SpectraMax spectrophotometer. Results were retrieved by SoftMax pro 6.2.1 software.

3.7 SDS-PAGE

SDS-PAGE was used to analyze the protein composition of the isolated fractions. This method separates proteins in a sample according to their molecular weight. A Bolt 10% Bis-Tris Plus precast acrylamide gel was used in this experiment, and the method was proceeded as stated in the manufacture protocol [51].

3.7.1 Sample preparation

Samples were prepared with sample buffer and reducing agent as presented in Table 3.7. The samples were heated for 10 minutes at 70°C and cooled down prior to loading.

Table 3.7: Sample preparation for SDS-PAGE with reagents and volumes. Sample volume was adjusted when equal amount of protein (µg) was loaded.

Reagent:	Volume:
Sample	13 µL
Bolt LDS Sample Buffer (4X)	5 µL
Bolt Reducing Agent (10X)	2 µL
Total Volume	20 µL

3.7.2 Electrophoresis

1X Running buffer was prepared by mixing 20 mL 20X Bolt MES SDS Running Buffer with 380 mL distilled water to get a final volume of 400 mL. The well-comb and tape cover on the precast gel cassette were carefully removed, and the gel was placed in a raised position in the Mini Gel Tank. 1X Running buffer was added to the chamber and the wells were washed three times with running buffer. SeeBlue Plus2 Prestained Standard (5 µL) and samples (20 µL) were loaded into the wells. The cassette was gently lowered and running buffer was added to the level of fill line. The apparatus was set at 200V for 22 minutes, or until the stain had reached the bottom.

3.8 Coomassie Brilliant Blue staining

After protein separation by SDS-PAGE the gel was placed in Coomassie Brilliant Blue (CBB) staining for 45 minutes. CBB is a dye used to stain proteins, this treatment allows for visualization of the proteins as blue bands in the gel. The gel was washed 5 minutes x 3 times with distilled water, and a destaining solution was added to the gel for 30 minutes. Destaining is used to get a clear background without destaining the protein bands. After 30 minutes a fresh destaining solution was added and the gel was left overnight or until the background was nearly clear. By the use of the program IrfanView 4.44 the gel was scanned with a white light scanner.

3.9 Western Blot

Western Blot (WB) was further used to confirm exosomal proteins present in the purified EV preparations. Tetraspanin CD9 is one of the proteins especially enriched in the membrane of exosomes, therefore the Anti-CD9 Antibody (rabbit anti-human) provided in the ExoAb Anitbody kit (SBI) was used to characterize exosomes.

3.9.1 Gel to membrane transfer

After SDS-PAGE the proteins were transferred from the gel to a nitrocellulose membrane in a Pierce G2 Fast Blotter machine. A nitrocellulose membrane and six filter papers were prepared and placed in transfer buffer with 10% methanol. A "sandwich" was made with three filter papers, membrane, gel and three filter papers, respectively. Transfer buffer was pipetted on top of the sandwich, and a roller was used to remove air bubbles to allow for a proper protein transfer. The Mixed Range MW (25-150kDa) program was selected.

3.9.2 Immunodetection

The membrane was blocked in blocking buffer (5% w/v skimmed milk in 1X TBS) for 50 minutes in room temperature on a shaker. Followed by 5 minutes x 3 times wash with 1X TBS. The Anti-CD9 Antibody (rabbit anti-human, System Biosciences) primary antibody (1Ab), was diluted in 5% w/v skimmed milk in 1X TBS to a 1:1000 dilution. The membrane was kept in 1Ab on a shaker overnight at 4°C. After 1Ab incubation the membrane was washed 5 minutes x 3 times with 1X TBS. The goat anti-rabbit HRP secondary antibody

(2Ab) was prepared as stated in the datasheet (1:20 000, System Biosciences). The membrane was incubated in 2Ab for 1.5 hours at room temperature on a shaker. Next the membrane was washed 5 minutes x 3 times in 1X TBS. The washing steps were performed, thereby removing any unbound antibodies, which would result in high background noise.

3.9.3 Chemiluminescence detection

Enhanced chemiluminescence (ECL) solutions ECL1 (500μL 2M Tris-HCl, 100μL luminol, 100μL p-coumaracid, 9.3mL distilled water) and ECL 2 (500μL 2M Tris-HCl, 6.1μL H_2O_2, 9.5mL distilled water) were prepared. The ECL1 is light sensitive and was therefore covered in aluminum. The two ECL solutions were mixed and the blot was kept in the solution for 1 minute. By the use of a Chemidoc imager (Bio-Rad) the colorimetric and chemiluminescence blot was visualized. Image Lab (Bio-Rad) software was further used to edit and export the blot image.

3.10 BBB Cell culture

The Blood-Brain Barrier hCMEC/D3 Cell Line was used in this study to investigate the permeability when exposed of endogenous exosomes. The human brain endothelial hCMEC/D3 cell line can easily be grown and used as a BBB model for studies on drug transport mechanisms with relevance to the CNS [52].

3.10.1 Aseptic technique

To prevent contamination of the cell culture all techniques were performed according to aseptic technique. The cell culturing was conducted in a clean lab area for cell and tissue culturing. Proper personal protection gear was used for further protection; shoe covers, gloves and lab coat. Hands were washed before and after cell culture work, and gloves were disinfected with 70% ethanol. All sterile work was performed inside a flow hood, which was sterilized before and after use by 70% ethanol and ultraviolet light. Media spillage was immediately cleaned up by 70% ethanol. All reagents, media and other solutions were sterilized before being used in the hood. Caps were left on every bottle until use and put back on as soon as possible to prevent contamination. Waste in contact with media was autoclaved to inactivate antibiotics and gene modified organisms.

3.10.2 hCMEC/D3 Medium Preparation

The endothelial cells were cultured in EndoGRO Basal Medium supplemented with EndoGRO-MV Supplement Kit and 1 ng/mL FGF-2 (Table 3.10). This medium is optimized for culture of human endothelial cells in a 5% serum environment. It contains no phenol red or antimicrobials which can cause cell stress and other effects that might influence experimental results. When medium was needed, 50 mL was transferred to a sterile conical tube. This was done to avoid warming of the entire bottle that can lead to degradation and reduced shelf life. The medium bottle has a special UV protective packaging therefore the conical tube should be covered by aluminum.

Table 3.10: The medium was provided as a kit including basal media and a supplement kit; containing supplements and growth factors unique for endothelial cells. The medium was prepared as stated in the product manual, and supplemented with FGF-2 [53].

Components	Volume	Final concentration in medium	Storage
EndoGRO^{TM} Basal Medium	475 mL		2-8°C
EndoGRO-LS Supplement	1.0 mL	0.2%	-20°C
rh EGF	0.5 mL	5 ng/mL	-20°C
Ascorbic Acid	0.5 mL	50 µg/mL	-20°C
L-Glutamine	25 mL	10 mM	-20°C
Hydrocortisone Hemisuccinate	0.5 mL	1.0 µg/mL	-20°C
Heparin Sulfate	0.5 mL	0.75 U/mL	-20°C
FBS	25 mL	5%	-20°C
FGF-2	1 mL	1 ng/mL	-20°C

3.10.3 ECM coating of flasks

Collagen type 1 is a major component of the extracellular matrix (ECM), and is commonly used for coating flasks of endothelial cell cultures to enhance cell attachment and proliferation. Collagen Type 1, Rat Tail was thawed at room temperature and diluted in 1X PBS to get a final concentration of 10 µg/cm². 5 mL of the solution was used to coat one T75

flask. The flask containing the coating solution was left in the incubator (37°C) for at least 1 hour before use. After incubation the solution was aspirated just before plating the cells.

3.10.4 Thawing of cells

Cells were removed from liquid nitrogen and incubated in a water bath (37°C) until they were completely thawed. The outside of the vial was disinfected with 70% ethanol and placed in the flow hood. The cells were transferred to a sterile 15 mL conical tube without introducing any bubbles. 9 mL of prewarmed medium (37°C) was slowly added dropwise to the conical tube. The whole volume must not be added at once, this can lead to osmotic shock of the cells and consequently decreased cell viability. The cell suspension was gently mixed by slowly pipetting up and down. The tube was centrifugated for 3min at 900xg to pellet the cells, and the supernatant containing residual cryopreservatives (DMSO) was removed. Cells were resuspended in 2mL of prewarmed-medium. 10 mL medium was added to the pre-coated T75 tissue culture flask, the cell mixture was added, and the flask was incubated at 37°C in a 5% CO_2 incubator. Medium was exchanged with fresh pre-warmed medium the day after plating. Thereafter medium was exchanged with fresh medium every two or three days.

3.10.5 Subculturing of cells

When the cells were approximately 80% confluent they were dissociated with trypsin-EDTA. The medium was carefully removed, 5 mL of warm trypsin-EDTA was added and the flask was incubated at 37°C until complete detachment of cells (3 minutes). 8 mL pre-warmed medium was added, and the suspension was mixed by gently rotating the flask. The cell suspension was transferred to a 15 mL conical tube and centrifugated for 4 min at 900xg to pellet the cells. Supernatant was discarded, and the cell pellet was resuspended in 2 mL pre-warmed medium. The number of cells were counted using Muse Count & Viability Kit (Millipore) and Muse Cell Analyzer (Millipore). Cells were plated to desired density in a new collagen covered flasks.

3.10.6 Cryopreservation

For every passage, as much cells as possible were frozen down in hCMEC/D3 medium containing 10% DMSO by the use of a Mr. Frosty Freezing Container. The protocol states that the cell line can be passaged for at least 10 passages without affecting the functionality,

therefore it is crucial to freeze down cells from early passages. The cell suspension was centrifuged for 4 min at 900xg and resuspended in freezing media. Cells were transferred to freezing tubes, placed in the freezing container and frozen down at -80°C. The next day the cells were transferred from the -80°C freezer to liquid nitrogen for long term storage.

3.10.7 BBB hCMEC/D3 cells exposed to endogenous exosomes

Cells were seeded on a pre-coated 6-well plate and grown until 80% confluency. The effect of concentration on the permeability was tested by adding both 10 µl and 40 µl exosomes (in PBS) to the cells. The plate was incubated for 1 hour at 37°C and at 5% CO_2. The medium (supernatant) was transferred to a 2 mL tube and was supposed to be analyzed by MS to verify exosome uptake by the cells. However, due to problems with the MS machine and limited time, the MS analysis was not performed.

3.11 Mass spectrometry

Mass spectrometry (MS) is a method that can be used for characterization of a wide range of biological molecules. The method involves ionization of a sample and measure of mass-to-charge ratio of the resulting ions. Both organic and inorganic samples can be analyzed, and the mass spectrometer gives qualitative and quantitative information on the molecular composition [54]. However, the quality of the mass spectra is dependent on sample purity and amount of sample [55]. The mass spectrometer consists of an ion source, a mass analyzer, a detection system and a computer system that can process the data. After ionization the beam of ions is directed into the mass analyzer, which will separate the ions based on m/z (mass/charge number of ions) [54].

3.11.1 In-Gel Tryptic Digestion

MS can be used for characterization of exosomes by identifying exosomal proteins. First the proteins were separated by SDS-PAGE and stained by CBB, then a band of interest was cut out for further analysis. Thermo Scientific™ In-Gel Tryptic Digestion Kit was used to perform digestion of the protein band, and the method was conducted as stated in the kit protocol [56]. In-gel digestion is a standard method used to prepare proteins for MS analysis. The essential steps in the In-Gel digestion are destaining, reduction, alkylation, digestion (enzymatic cleavage of proteins into peptides) and extraction. The gel pieces are destained by

incubation in an organic solvent, this results in release of the CBB molecules bound to the protein [55]. To improve digestion and sequence coverage the disulfide bridges are reduced to disrupt the tertiary structure. Breaking the disulfide bonds facilitates protein unfolding and consequently improved digestion of the protein. To prevent unwanted reactions during analysis the highly reactive sulfhydryl groups in the protein are blocked by alkylation [57]. To generate peptides, the serine protease trypsin is frequently used for enzymatic cleavage of the protein. Trypsin specifically cleaves the peptide bonds after the carboxyl group of lysine and arginine.

3.11.2 Reversed-phase high-performance liquid chromatography (RP-HPLC)

After isolation of the peptides, the sample was further purified and concentrated by the use of reversed-phase chromatography. Pierce® C18 Spin Columns and the attached protocol [58] was used to perform the sample clean-up. The spin column contains C18 reversed-phase resin as a stationary phase, and by the use of a more polar mobile phase (acetonitrile) the hydrophobic molecules in the polar mobile phase will be absorbed by the stationary phase. This results in elution of the hydrophilic molecules first; like salts, buffers and other interfering contaminants, while the peptides are bound to the stationary phase. After the washing step, the sample was eluted from the stationary phase and gently dried in a vacuum evaporator. The pellet was suspended in 10 μL 0.1% formic acid and frozen down until MS-analysis.

3.12 Isolation of primary porcine brain microvascular endothelial cells

Primary cell cultures of brain endothelial cells represent the best phenotype to the *in vivo* BBB [59]. Porcine brain endothelial cells (PBECs) are proven to retain their BBB characteristics in culture and give higher transendothelial electrical resistance (TEER) compared to brain endothelial cells from other species [60]. In addition, the porcine anatomy, genome and disease progression are comparable to humans. Pig brains are more ethically acceptable to use in research and they are considered a by-product from the industry [60].

PBECs were isolated, however the investigation of exosome uptake in these cells was not assessed due to limited time. All techniques were performed according to aseptic technique,

and equipment was autoclaved prior to isolation. Media, enzymes and other solutions were prepared one day in advance. Pig brains were picked up from the local slaughterhouse and stored on ice until isolation of primary cells.

3.12.1 Removing the meninges

The flow hood was covered in tissue paper to avoid excessive cleaning. Two 1 L beakers with PBS were placed on ice inside the flow hood. Where one beaker was for washing, and the other one for storage of the brain after removing meninges. The brain was gently washed in the washing beaker, and the meninges were removed with a fine-tip curved forceps and placed in a petri dish. The clean brain was transferred to the storage beaker. The procedure was repeated with all of the brains and the petri dish with the meninges was discarded.

3.12.2 Isolating the grey matter

A petri dish containing 5-10 mL media and a 500 mL flask were placed on ice inside the hood. As much grey matter as possible was scraped off the brains with a sterile scalpel. White matter was avoided in the process and meninges left on the brain were removed by the forceps. The grey matter was transferred to the petri dish with media, and when full the content was transferred to the 500 mL flask. This was repeated with all the brains and the remains of the brains were discarded after this step.

3.12.3 Liquid homogenizing

A 500 mL cell culture flask was placed on ice. The solution was homogenized by the use of a douncer cell homogenizer, also known as a tissue grinder. The douncer consists of two different size pestles, one loose pestle and one tight pestle. The grey matter solution was transferred to the grinder tube and homogenized with the loose pestle (8 down and up strokes). The looser fit works well to create a homogenous sample. Then the homogenous sample was grinded by the tight pestle, which allows for maximum friction and cell disruption. The homogenate was transferred to the 500 mL cell-flask and the method was repeated with the rest of the material. If the homogenizing was too difficult the material was diluted with media. When all the material was homogenized the homogenate was diluted to approximately 450 mL with media.

3.12.4 Filtration and digestion

The homogenate was filtered. After filtration of 50 mL homogenate, the filter was washed with media and placed in a petri dish with digestion media. This was repeated with all of the homogenate and the filters were incubated in digestion media for 1 hour at 37°C on a shaker. After incubation the filters were washed with media until clean.

3.12.5 Centrifugation

The solution was transferred to two 50 mL tubes, the petri dish was washed with 10 mL media, and equal volume was transferred to the tubes. The tubes were centrifugated for 5 min, 250 g at 4°C, and the supernatant was discarded. Each cell pellet was resuspended in 10 mL media, followed by an additional 20 mL media. The centrifugation step and resuspension were repeated once more. After resuspension, the tubes were incubated on ice for 5 minutes. The supernatant was carefully removed and transferred into two new 50 mL tubes.

3.12.6 Cryopreservation

The tubes were centrifuged for 5 min, 250 g at 4°C. Supernatant was discarded, and the pellet was resuspended in 7-9 mL freezing media. The cell suspension was transferred to cryo-tubes, placed in an iso-propanol filled freezing box and frozen down at -80°C overnight. Next day the cells were moved to liquid nitrogen for long-term storage.

3.13 Primary rat astrocyte culture

Astrocytes are the most abundant type of glia cell in the CNS. They contribute to many essential functions in the CNS including maintenance of the BBB [61]. In order to maintain the *in vivo* BBB phenotype of brain endothelial cells, they are often co-cultured with astrocytes to preserve tight junctions [62]. Primary rat astrocytes from Denmark were cultured and all techniques were performed according to aseptic technique.

Poly-L-lysine was diluted in sterile water (10 µg/mL), sterile filtered and used as a coating solution. A 12-well plate with coverslips was coated (1 mL per well) and incubated for 1 hour at 37°C. The coating solution was removed, and the plate was left to dry for 1 hour in the hood. Astrocyte culture medium was prepared (500 mL DMEM, 10% FBS, 1% pen-strep) and

warmed up to 37°C in a water bath. A vial of primary rat astrocytes was thawed rapidly in a water bath and added dropwise to the culture medium. 1 mL of the cell suspension (50 000 cells) was added to each well and incubated at 37°C in a 5% CO_2 incubator. Medium was changed the next day to remove DMSO, thereafter the medium was changed every two days until 70% confluent.

3.14 Confocal microscopy

Laser scanning confocal microscopy is a form of fluorescence microscopy where a laser beam is focused on a small area of a sample, building up an image by collecting the emitted photons from the fluorophores [63]. This method allows for visualization within both living and fixed cells by the use of optical sectioning, providing three-dimensional data by collecting multiple focal planes in a z-stack [64].

For analysis of exosome uptake in rat astrocytes, both the cells and exosomes were stained with fluorescence dyes and images were taken by the Nikon A1 / A1R Confocal Laser Microscope System using a 60X oil objective. VECTASHIELD Antifade Mounting Medium (with DAPI) was used, and it has the feature to prevent rapid photobleaching of fluorescent dyes. The mounting medium also contains the nuclear stain DAPI that can pass through an intact cell membrane and emit blue fluorescence when bound to DNA. Fluorescence images of WGA640 and DAPI stained astrocytes were acquired at 642/662 nm and 358/461 nm. Images of WGA488 stained exosomes were acquired at 490/515 nm. The lasers used in this experiment are presented in Table 3.14. The negative control was a slide with stained astrocytes, positive control was a slide with stained exosomes, and the blank had no cells and no exosomes. All images were acquired using the same laser intensities and detection settings. Images were captured by the NIS-Elements imaging software (Nikon).

Table 3.14: Fluorescence dyes, Ex/Em and lasers used in the analysis.

Dye	Excitation	Emission	Laser
WGA640 – cell membrane	642 nm	662 nm	640 nm
DAPI - nucleus	358 nm	461 nm	408 nm
WGA488 - exosomes	490 nm	515 nm	488 nm

3.14.1 Staining of exosomes

Three isolated exosome fractions (1.5 mL) with similar sizes were joined to achieve a higher concentration of exosomes. The exosomes were pelleted for 1 hour, 16 xrp at 4°C. The supernatant was removed, and the pellet was resuspended and incubated in WGA488 stain (5 µg/mL, diluted in HBSS) for 30 minutes, dark at room temperature. After incubation the exosomes were centrifugated for 30 min, 16 xrp at 4°C. Supernatant was removed, and the stained exosomes were washed twice with PBS+. The pellet was diluted in 0.5 mL PBEC Assay (HBSS, 25mM HEPES, 0.5% BSA). To confirm successfully staining of exosomes, the fluorescence was measured by SpectraMax at 490/515 nm.

3.14.2 Rat astrocytes incubated with exosomes

Rat astrocytes were grown on pre-coated coverslips in a 12-well plate until 70% confluent. The medium was removed, and the astrocytes were stained by WGA640 (20ug/mL, diluted in HBSS) for 10 minutes. HBSS was used to wash the cells three times. 0.5 mL pre-stained exosomes were added to each well and incubated with the cells for 20 minutes. The coverslip was washed two times with 4% paraformaldehyde (PFA) and left to dry in order to fix the cells. 8 µl mounting medium (Vectashield, Antifade Mounting Medium with DAPI) was added to the microscope slide and the coverslip was placed cell side down on the slide. Mounted slides were stored dark at 4°C until use.

4. Results

4.1 Determination of size and homogeneity of vesicle fractions

Endogenous exosomes from blood plasma were separated from apoptotic bodies and micro-vesicles by size exclusion chromatography (SEC) as described in section 3.2. SEC has been shown to isolate exosomes from blood plasma without significant impurities and with a low albumin contamination. DLS (Malvern, UK) was applied (section 3.3) to determine the vesicle size by intensity, z-average diameter and homogeneity of the fractions. Vesicles ranging from 50-100 nm in diameter were considered as exosome fractions. The measurements all passed the instrument quality requirements. Size measurements were repeated multiple times (n >10) with different isolates.

Size distribution of isolated fractions (F7-F13) is shown in Figure 4.1. Although the manual collection of fractions was expected to introduce some variability, the size of the different fractions was observed to be similar in all isolations. Fraction 10, 11 and 12 were constantly observed with a diameter of 60-90 nm, indicating that these may be the best fractions for further exosome identification. F13 was often observed with an irregular graph indicating low homogeneity and contamination of the sample. However, it had the size of an exosome fraction and was included in further analysis. Fraction 7, 8 and 9 were continuously measured to have a size above 100 nm and were not considered exosome fractions. Most of the fractions repeatedly showed a second peak at around 5560 d.nm this may be due to contamination of the vesicle fractions.
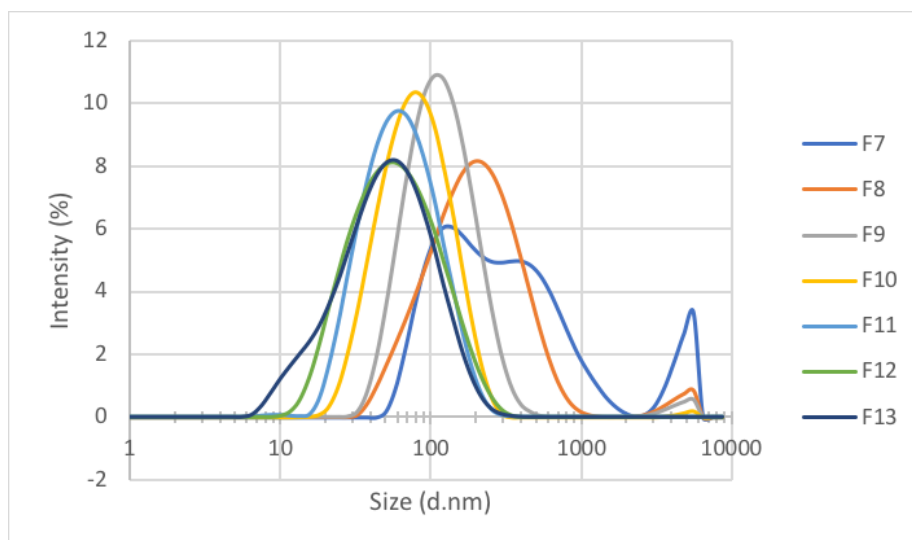
Figure 4.1: Particle size by intensity of isolated fractions as measured by DLS. Size (d.nm) by intensity (%) of recovered exosomes in each fraction (F).

Z-average diameter and poly-dispersity (PDI) values of the fractions were retrieved from the Zetasizer software. The mean and standard deviation (SD) was calculated, and all data is shown in Table 4.1. From these results only F10 and F11 are measured with a particle diameter within 50-100 nm. Fractions 9-13 had low average PDI of around 0.2, indicating high particle homogeneity in these vesicle fractions. This reveal that F10 and F11 can be considered as exosome fractions with high particle homogeneity. Both the size distribution and z-average indicated that fraction 7, 8 and 9 had a diameter above 100 nm. After several experiments (n > 5), it was concluded that these fractions were not exosome fractions and they were excluded from further studies.

Table 4.1: Average size and poly-dispersity of isolated (PDI) vesicle fractions retrieved from the Zetasizer software. SD was calculated.

Fraction	Average size (Z-Average, d.nm)	Average PDI
7	233,333 ± 5,675	0,549 ± 0,085
8	166,067 ± 3,726	0,314 ± 0,040
9	104,567 ± 0,759	0,222 ± 0,006
10	69,487 ± 0,348	0,209 ± 0,010
11	54,560 ± 0,118	0,212 ± 0,005
12	48,627 ± 0,123	0,261 ± 0,003
13	41,227 ± 0,095	0,291 ± 0,003

4.2 Detection of protein contamination and use of ultrafiltration for removal

Although the qEV SEC column is proposed to isolate EVs with low protein levels, the size distribution results (Figure 4.1) suggest that the vesicles may be contaminated. Isolation of exosomes from blood plasma is difficult due to highly abundant proteins and other impurities, where the most dominating protein is albumin (66.5 kDa). First, the total protein concentration was measured in order to assess the protein contamination of isolated fractions. Total protein was measured by BCA Protein Assay as described in section 3.6.1. The fractions considered as exosome fractions (10, 11, 12 and 13) were analyzed, and the mean result of the total protein measurement is presented in Figure 4.2. The protein level was expected to increase by every collected fraction, due to the fact that serum proteins elute slower than EVs. As expected, high level of contaminating protein is detected in fraction 13. Fraction 10 was observed with lowest protein contamination. Furthermore, there is a relatively higher amount of protein in F12 compared to F11, this would suggest that most of the serum proteins are eluted from fraction 12-13. The product manual states that serum proteins are predominantly eluting in fraction 11-13 [65], however, in this experiment serum proteins are not observed to elute until fraction 12.
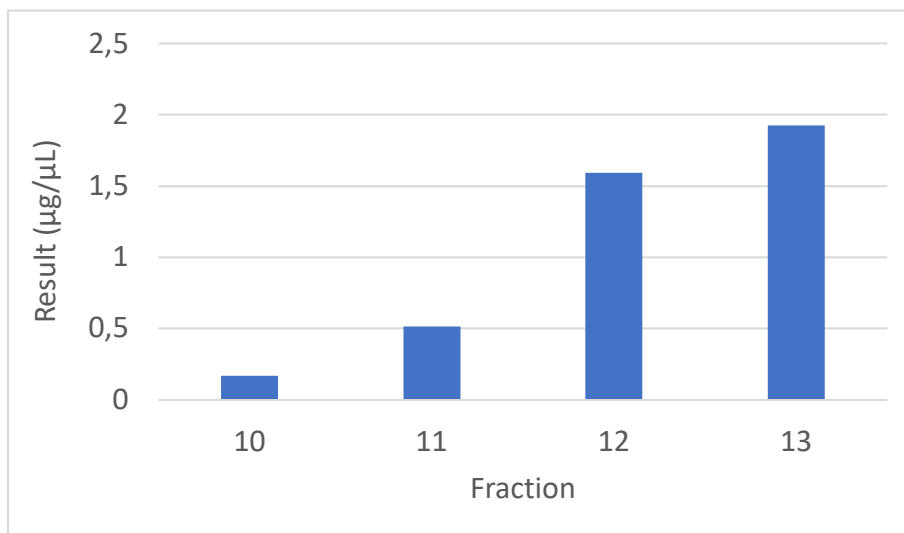

Figure 4.2: Total protein concentration in μg/μL of the vesicle fractions measured by BCA Protein Assay.

For further analyzation of protein composition, the EV isolates were separated by SDS-PAGE on a Bolt Bis-Tris Plus precast acrylamide gel (section 2.3, Thermo Scientific User Manual [51]) and stained by CBB (section 3.8). The protein content of isolated vesicle fractions is shown in Figure 4.3. One gel was loaded with equal volume of sample (4.3A) in order to compare the protein amount in the different vesicle fractions. This revealed that F13 (Figure 4.1, dark blue line) was the sample with highest protein contamination, showing high expression at ~ 62 kDa. F10 (Figure 4.1, yellow line) was observed to be the sample with lowest protein contamination. These results correlate well with the total protein amount measured by BCA.

Moreover, the vesicle fractions were lysed in order to compare the protein composition to the non-treated samples. 10 µg protein was loaded and the protein separation is shown in Figure 4.3B. Lysed samples (sample 2,4 and 6) had the same intensity and number of protein bands as the non-treated samples (sample 1,3 and 5). This would suggest that the lysis may not extract enough protein to be visualized in the gel, or that the lysis was not complete. Further analyzation should be done to determine the effect of lysis on the vesicle fractions.

Vesicle fractions were observed to be highly contaminated by proteins, and with this in mind, ultrafiltration (section 3.4, Millipore User Manual [50]) was tested as a method to remove residual protein. Both the 3K and 100K filter devices were tested for removal of macromolecular components and the samples were compared to non-filtrated vesicle fractions. A comparison of non-filtrated fractions and 3K filtrated fractions is shown in Figure 4.3B. Where sample 1 and 2 are non-filtrated, and sample 3,4,5 and 6 are filtrated by a 3K device (4X). No substantial difference was observed when comparing the protein bands of the non-filtrated samples and the 3K filtrated samples. Only one protein at ~98 kDa was observed to be removed by the 3K device. This would suggest that 4X concentration by a 3K filter device is not able to eliminate all the protein contamination of the vesicle fractions. This was expected as most proteins are bigger than 3 kDa and hence be retained by the 3K filter.

For further analyzation of protein removal, fraction 13 was ultrafiltrated by the 100K filter device and the result is presented in Figure 4.3C. Fraction 13 was used as this was the fraction with highest protein concentration. In contrast to the 3K filter, the 100K filter was observed to remove a high amount of protein from the vesicle fraction. Most notably proteins with a molecular mass of ~ 62 kDa, indicating that this is a suitable method for albumin removal.

From these results the 100K filter device was observed to be the best method for residual protein removal.
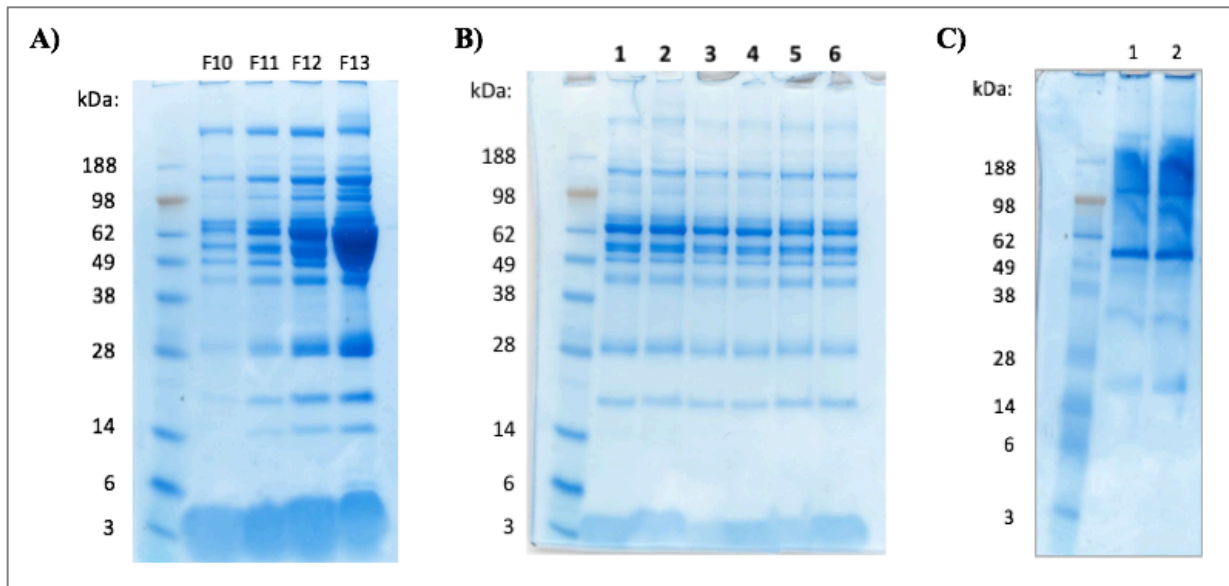

Figure 4.3: Protein separation of isolated exosomes. (**A**) 26 µl of each vesicle fraction was loaded to compare the protein amount in the different vesicle fractions. (**B**) 10 µg protein loaded. 1=F12 non-lysed(1X), 2=F12 lysed(1X), 3=F12 non-lysed(3K filter, 4X), 4=F12 lysed(3K filter, 4X), 5=F11 non-lysed(3K filter, 4X) and 6=F11 lysed(3K filter, 4X). (**C**) Sample 1-2=F13 ultrafiltrated by a 100K device (26X).

Further testing was done in order to verify residual protein removal by ultrafiltration (100K). NanoDrop (Thermo Scientific, U.S.A) was used to measure the total protein amount of the F13 sample before and after ultrafiltration. BCA Protein Assay would be a better approach to measure the total protein amount, however BCA was not possible in this analysis due to the low filtrate volume. As expected, the results show a considerable reduction in protein content after ultrafiltration (Table 4.2). The ultrafiltration resulted in a concentration factor of 26, with this in mind the estimated concentration would be 36.192 mg/mL. However, the protein amount was measured to be 9.238 mg/mL, which is a 74% reduction in protein. This result further demonstrates that 100K ultrafiltration is the preferable method in order to remove residual protein.

Table 4.2: Protein quantification by NanoDrop. Total protein amount (mg/mL) of fraction 13 was determined before and after ultrafiltration by Amicon 100K filter device. The sample was centrifuged 10 minutes resulting in a concentration factor of 26.

Sample	mg/mL	A280
F13 Before concentration (1X)	1.392	1.39
F13 After concentration (26X)	9.238	9.24

As an additional verification, DLS was applied to analyze the effect of ultrafiltration on the size distribution. The vesicle fraction (F13) was analyzed directly after isolation, after thawing and after ultrafiltration as presented in Figure 4.4. The size distribution results confirm that ultrafiltration did remove the contamination detected at 5560 d.nm. All of these experiments would suggest that ultrafiltration by a 100K device is a suitable method for residual protein removal of vesicle fractions. Another interesting finding was that the thawed sample had a peak at ~24 d.nm, this may indicate that exosomes are degraded and affected by freezing and thawing.
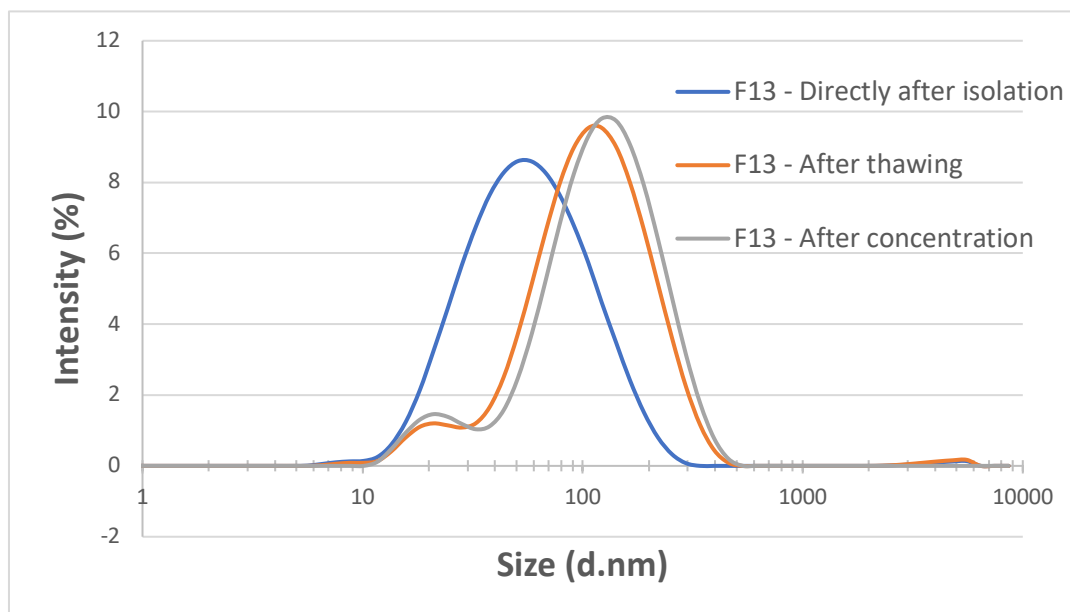

Figure 4.4: Size distribution by intensity measured by DLS. Fraction 13 was analyzed directly after isolation, after freezing/thawing, and after concentration by Amicon Ultra filter (Conc.factor 26X).

4.3 Influence of storage condition on exosomes

During size distribution analysis the samples showed signs of degradation after freezing and thawing. Therefore, different storage conditions were tested in order to keep the exosomes stable until use. Exosomes were isolated by SEC and analyzed by DLS. Amicon Ultra filter 100K was used to concentrate the samples (9X) and remove protein contamination. After concentration the samples were analyzed by DLS again, followed by storage at different temperatures. Storage temperatures tested were 20°C, 4°C and -20°C (room temperature). The samples were analyzed 1-3 days after storage at the specific temperature. The size distribution analysis is presented in Figure 4.5. Storage for three days at 20°C showed no degradation of the vesicle fraction. And interestingly, the sample stored at -20°C did not show any signs of degradation after multiple thawing. Previously reported size distribution indicated that the exosomes may be affected by freezing and thawing (Figure 4.4). However, in this analysis the sample stored at 4 °C was the most affected sample as the intensity was lower on day three. These results suggest that room temperature (20°C) and -20°C would be the best storage temperatures for exosomes.
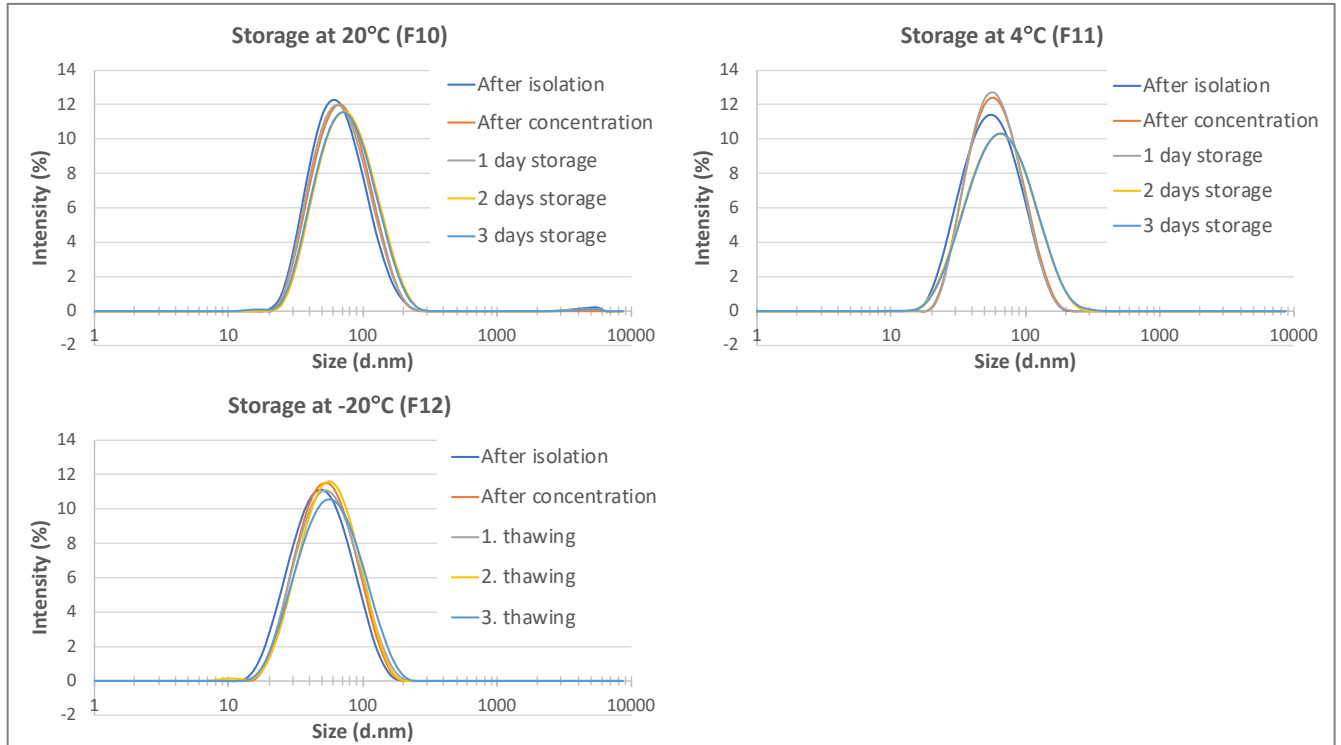

Figure 4.5: Size distribution by intensity of fractions after isolation, after concentration (9X) and after 1-3 days storage at the specific temperature. Storage temperatures were 20°C, 4°C and -20°C.

For further testing of best storage conditions, aliquots of one fraction (F11) was placed at the following temperatures 20°C, 4°C, -20°C and -80°C. The fraction was not ultrafiltrated in this analysis. Size distribution was analyzed by DLS after isolation and storage, and the results are shown in Figure 4.6 (Z-average diameter and PDI values are presented in Table 1-4 in Appendix). In this experiment, multiple freezing and thawing cycles were found to affect the exosomes drastically. Where -20°C was observed to cause more and faster degradation compared to -80°C. This would indicate that exosomes need to be aliquoted prior to freezing in order to prevent degradation. The sample stored in room temperature (20°C) showed no signs of degradation after three days, but on the eight day, size was measured to be above 100 d.nm indicating degradation. This would suggest that samples can be stored in room temperature for three days without being affected. 4°C was observed to be the best storage condition in this experiment. After eight days the size distribution is relatively similar only with a lower intensity.
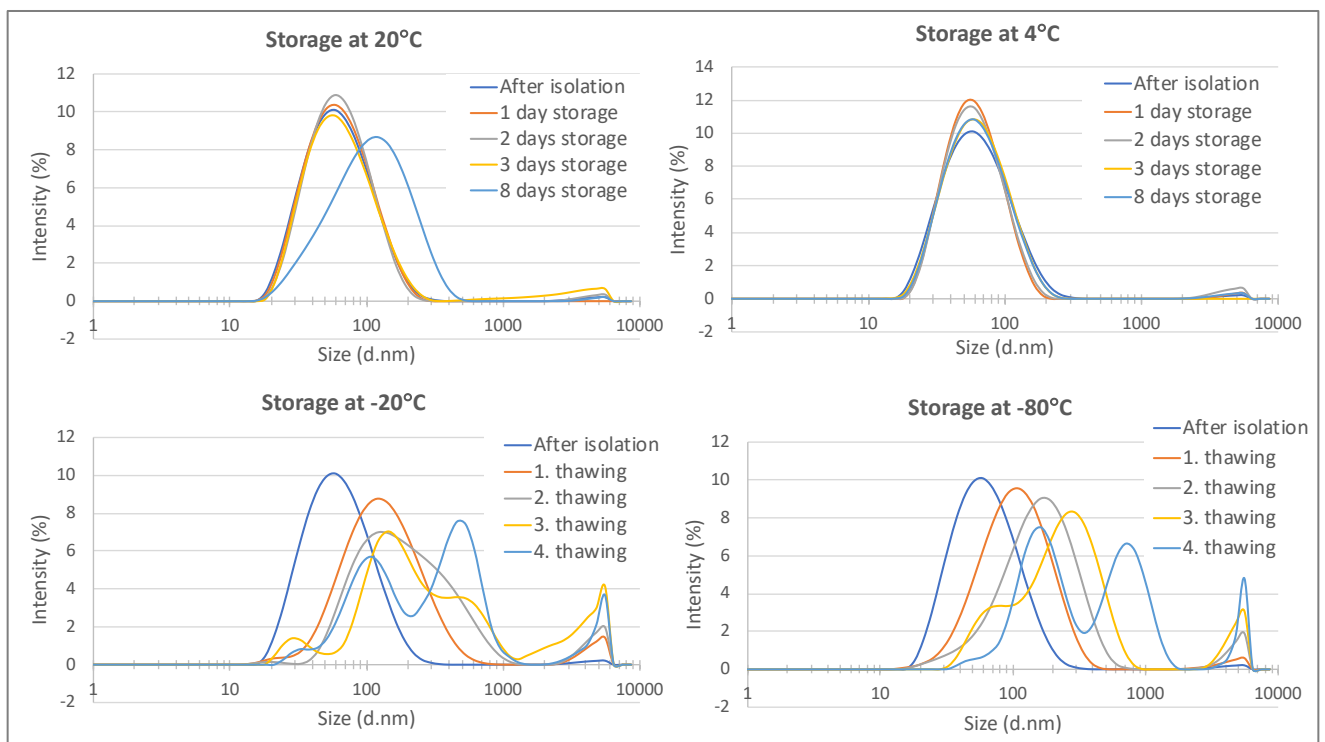

Figure 4.6: Size distribution by intensity of fraction after isolation and after 1-8 days storage at the specific temperature. Storage temperatures were 20°C, 4°C, -20°C and -80°C.

Absorbance of the vesicle fraction was measured after isolation and storage to determine if protein (280 nm) and lipid (498 nm) content were altered at different storage conditions. The

favorable composition would be constant lipid concentration with low protein contamination, indicating that the exosomes are kept intact without degradation. The protein and lipid content after storage are presented in Figure 4.7. At 20°C the lipid and protein content are observed to be almost constant during the days of storage. The highest protein values are measured in the sample stored at -80°C. Lipid content was measured highest on day three in the 4°C and -20°C sample. This analysis demonstrates that short-term storage at 20°C or 4°C would be the best condition in order to preserve the exosomes. The fact that protein and lipid contents are altered during storage suggest that exosomes preferably should be studied directly after isolation with no long-term storage.
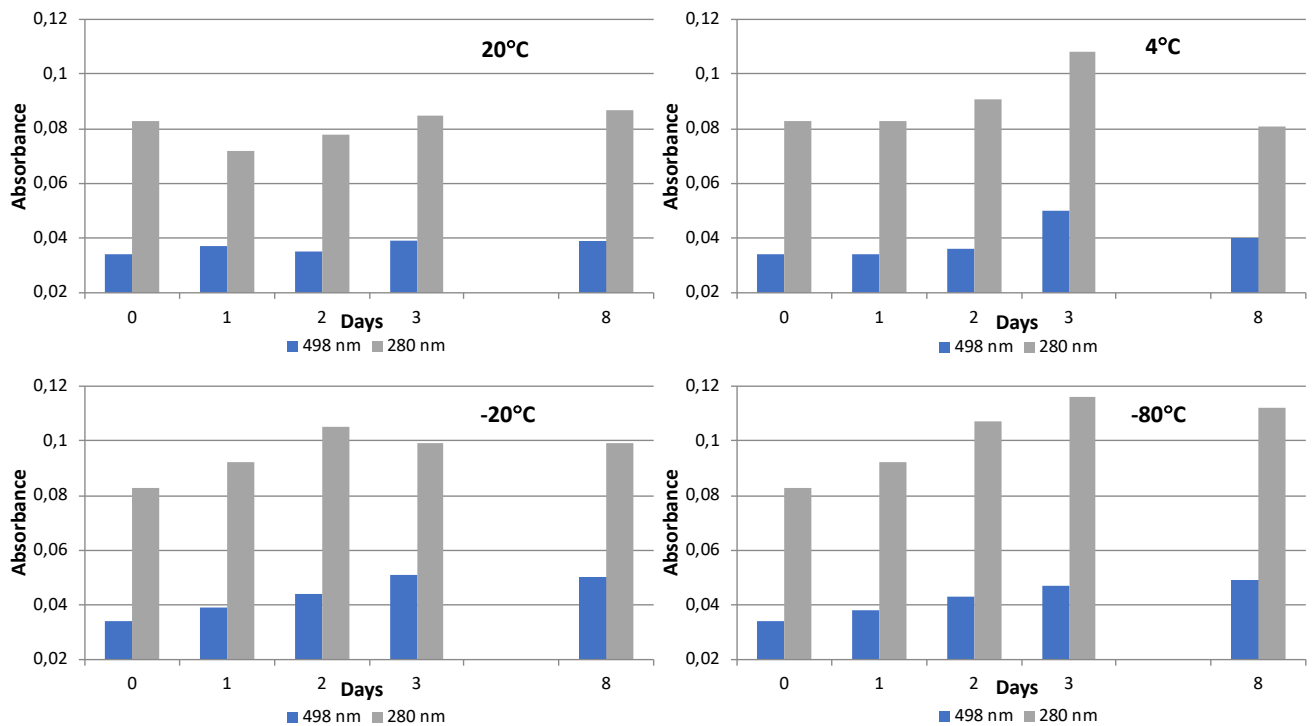

Figure 4.7: Absorbance measurement of fractions after isolation and after storage at the specific temperature. Where day 0 present the measurement after isolation. Protein was measured at 280 nm and lipid at 498 nm.

4.4 Detection of abundant proteins in exosome fractions by MS

Mass spectroscopy (MS) was applied to characterize exosomes by identifying exosomal proteins in the isolated vesicle fractions. Non-ultrafiltrated fraction 10,11,12 and 13 were separated by SDS-PAGE and stained by CBB (Figure 4.8A). Four bands suspected to contain exosome specific proteins, were cut out from the gel (Figure 4.8B). The protein bands were processed by in-gel digestion (section 3.11.1, Thermo Scientific [56]) and purified by reversed-phase chromatography (section 3.11.2, Thermo Scientific [58]) prior to MS analysis.
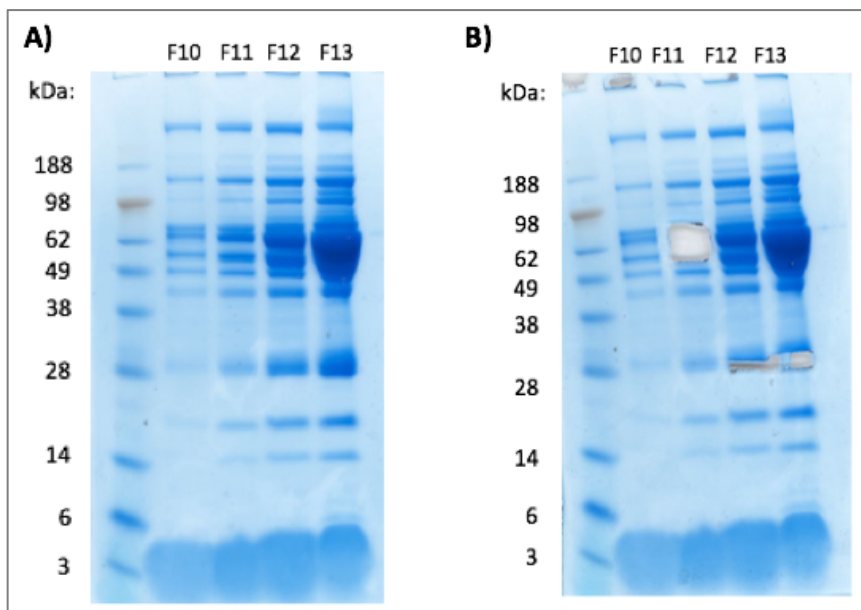

Figure 4.8: Protein composition of isolated vesicle fractions. (**A**) Samples (26 μl) separated on a Bolt Bis-Tris Plus precast acrylamide gel. (**B**) The same gel after cutting out bands of interest for further analysis by MS.

In the MS analysis immunoglobulin and fibrinogen beta were identified as highly abundant proteins, and details from the MS analysis are presented in Table 4.3. The identification of highly abundant proteins in plasma would indicate that the samples were not pure enough prior to MS. Suggesting that ultrafiltration of vesicle fractions may be needed in order to remove interfering proteins. Exosome specific proteins were expected to be in the protein bands, nevertheless they were not detected in the MS analysis. The concentration of exosomal proteins was expected to be low and hence be difficult to detect by CBB. These results would suggest that exosomal proteins may not be present in the bands of interest, the fractions are too contaminated or that too low amount of sample was applied in the analysis. Further investigation is needed in order to identify exosomes by MS.

Table 4.3: Identified proteins in MS analysis.

Identified protein	Accession number	Detected m/z signal and charge state	De novo sequenced protein fragment	Retention time (RT) / Scan (S)
Immunoglobulin IgM heavy chain (63 kDa)	P0DOX6	625.3108/+2 515.2847/+2 693.91425/+2 587.35754/+2	QATGFSPR QIQVSWLR NVPLPVIAELPPK PLPVIAELPPK	RT=18.104874/S=680 RT=21.261759/S=842 RT=22.048676/S=883 RT=22.474434/S=904
Fibrinogen beta (55kDa)	P02675	802.3373/+2 516.77435/+2 776.83124/+2 842.85474/+2	LESDVSAKFEYC IRPFFPQQ HEDDNEEGFFSAR YYWGGQYTWDFAK	RT=15.478409/S=541 RT=19.014816/S=724 RT=20.986893/S=825 RT=22.08725/S=887

4.5 Identification of the exosome specific marker, tetraspanin CD9

CD9 is a low abundant protein in the vesicle fractions making MS a difficult identification method. The complex mixture of different proteins also complicates the mass spectrum analysis. Therefore, western blotting (WB) was applied in order to confirm the tetraspanin CD9 protein. Here, detection of low abundant proteins can be achieved by immunoprecipitation by the use of a specific antibody. The vesicle fractions (26 μl) were separated by SDS-PAGE and immunoblotting was subjected to immunodetection with the tetraspanin CD9 antibody (System Biosciences, ExoAb Antibody Kit9) as described in section 3.9. By the use of a Chemidoc imager (Bio-Rad) a colorimetric image was taken (Figure 4.9A), and the chemiluminescence blot was visualized (Figure 4.9B). Image Lab (Bio-Rad) software was used to edit and export the blot image.

Tetraspanin CD9 showed high expression in the predicted height (28 kDa) on sample F13, indicating that exosomal proteins are present in this vesicle fraction. The protein was predicted to be present in all of the fractions, however none of the other fractions showed expression of CD9. Further investigation is needed in order to identify CD9 in all fractions expected to contain exosomes.
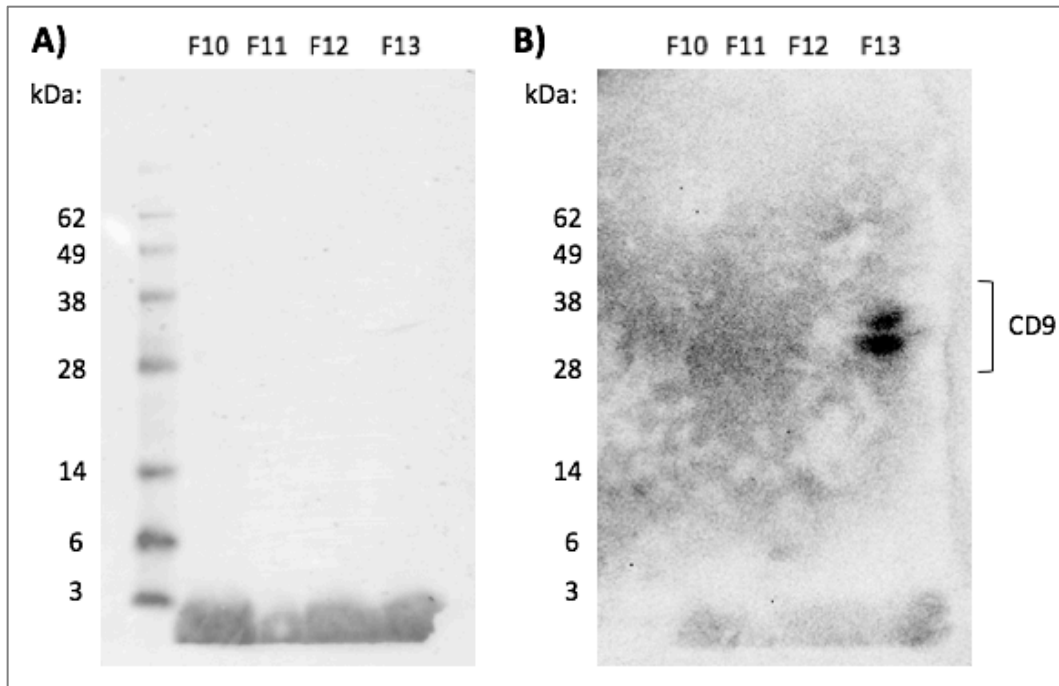
Figure 4.9: (**A**) Colorimetric image of the membrane after immunoblotting, showing the molecular weight ladder. (**B**) Chemiluminescence image of the same membrane. Anti-CD9 Antibody (rabbit anti-human) 1Ab diluted 1:1 000 and goat anti-rabbit HRP 2Ab diluted 1:20 000. Exosomes were identified in the F13 sample by the use of tetraspanin CD9 that are specially enriched in the membrane of exosomes.

4.6 BBB permeability of endogenous exosomes in BBB hCMEC/D3 cells

As exosomes have a potential ability to cross the BBB, the BBB hCMEC/D3 cell line (section 3.10) was exposed of endogenous exosomes to study the BBB permeability as described in section 3.10.7. The effect of concentration on the permeability was tested by adding different volumes of exosomes. However, due to problems with the MS machine and limited time, the MS analysis was not performed.

4.7 Investigation of exosome uptake in astrocytes by confocal microscopy

To investigate exosomes as a drug delivery system in neurological diseases, it is important to verify that exosomes are able to cross the BBB to deliver their cargo. Astrocytes are the most common cell type in the brain, contributing to many essential functions including development and maintenance of the BBB [61]. The exosome uptake mechanism by a recipient cell is cell-specific and still not unraveled. Therefore, it is important to establish exosome uptake by the BBB cells to confirm that drugs can be transported into the brain. Exosome uptake in rat astrocytes was studied by confocal microscopy (section 3.14). Rat astrocytes were cultured as described in section 3.13, after two days the cells were 70% confluent (Figure 4.10) and ready for incubation with exosomes (Z-average and PDI values of fraction are presented in Table 5 in Appendix). The incubation was performed as described in section 3.14.2.
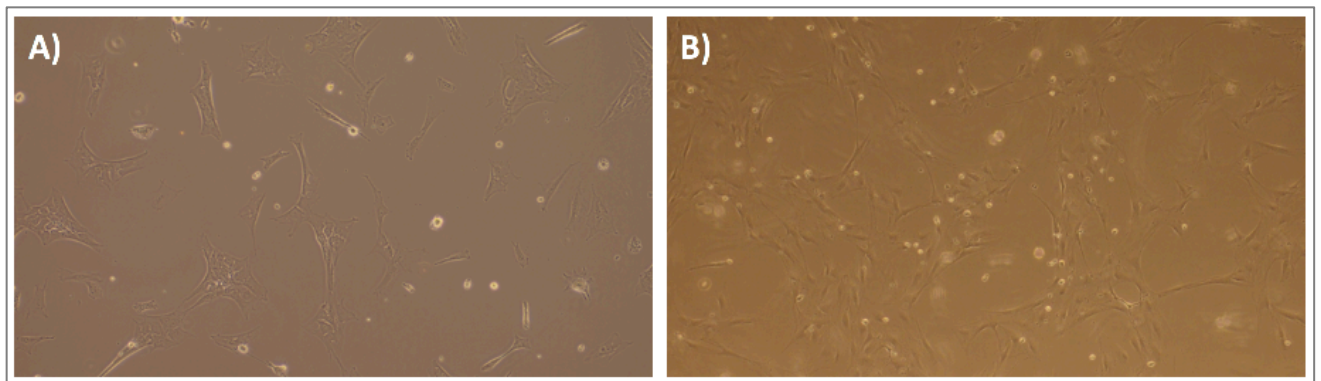

Figure 4.10: Cell culture of rat astrocytes. Images captured by a light microscope (Olympus CKX41, Germany) using a 10X object. (**A**) One day old astrocytes, 50 000 cells were seeded. (**B**) Two days old astrocytes, 70% confluent and ready for incubation with exosomes.

Fluorescence images of WGA640 and DAPI stained astrocytes were acquired at 642/662 nm and 358/461 nm. Images of WGA488 stained exosomes were acquired at 490/515 nm (section 3.14, Table 3.14). A blank without cells and exosomes, a negative control with stained astrocytes and a positive control with stained exosomes were used for comparison (Figure 4.11). The positive control was most frequently observed with few exosomes in the scan area (n > 10), however in some rare cases the exosomes were observed numerous and clumped together (n =2).
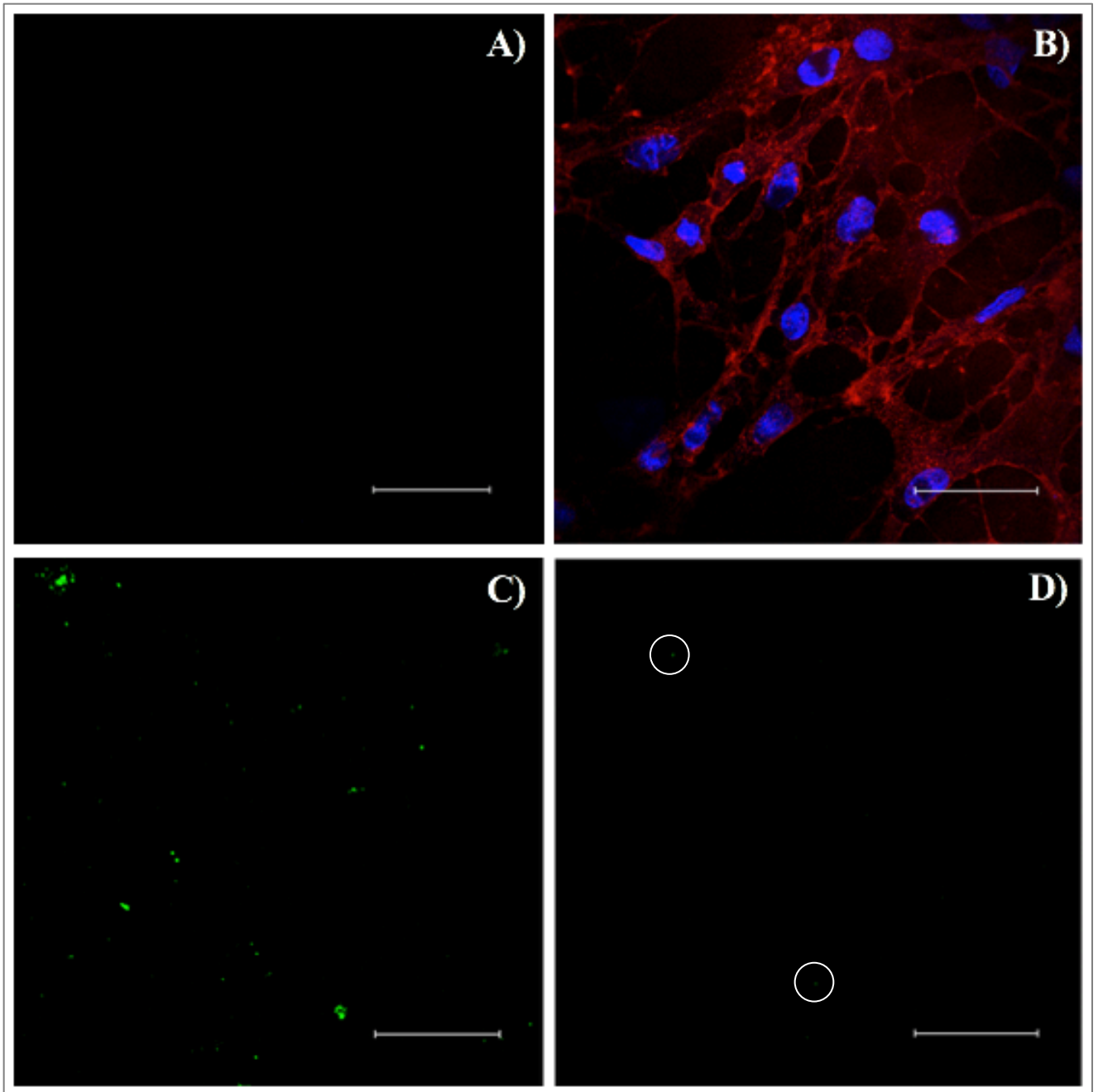
Figure 4.11: Controls used in the confocal experiment. (**A**) Blank, slide without cells and exosomes. Bar, 50 μm. (**B**) Negative control, WGA640 (red) and DAPI (blue) stained astrocytes. Bar, 50 μm. (**C**) Positive control, WGA488 (green) stained exosomes. Bar, 50 μm. (**D**) An additional image of the positive control. WGA488 (green) stained exosomes, indicated by circles. Bar, 50 μm. The positive control was observed with both numerous exosomes clumped together (C), but most frequently with only a few exosomes (D).

Astrocytes were incubated with exosomes for 20 minutes, and a single confocal scan of the components is shown in Figure 4.12. During the experiment exosomes were identified in around 80% of 30 scans. In the single confocal scan, three exosomes are visible close to the cells, but verification of exosome uptake was difficult with this type of image. Therefore, further investigation was done by capturing multiple focal planes in a z-stack to get a better understanding in if the exosomes actually are inside the astrocytes.
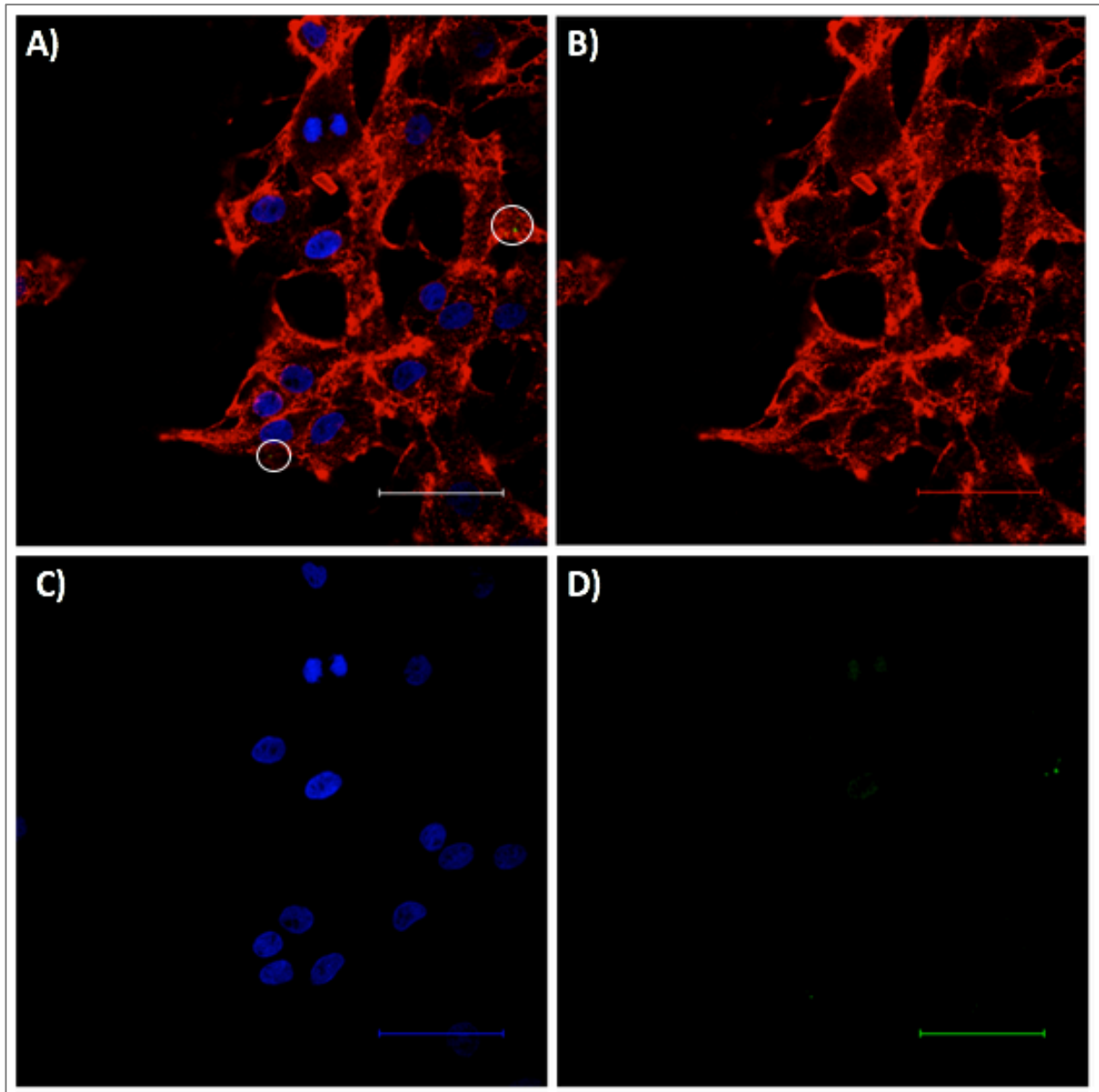

Figure 4.12: Single confocal scan of rat astrocytes incubated with exosomes for 20 min. (**A**) All channels, where exosomes (green) are marked with circles. Bar, 50 μm. (**B**) Red channel, astrocyte membranes. Bar, 50 μm. (**C**) Blue channel, nuclei. Bar, 50 μm. (**D**) Green channel, exosomes. Bar, 50 μm.

By collecting images at various focal planes, the entire sample volume can be visualized. A three-dimensional image of the cells based on multiple focal planes is shown in Figure 4.13. In total 14 exosomes are detected in the captured focal planes (indicated by circles). In stack 2 there are two exosomes that are not present in any of the other stacks (Figure 4.13B, indicated by a square), this area is blown up and presented in Figure 4.14. This may reveal that exosomes are present inside the astrocytes. Although this may be indication of exosome uptake by the cells, further investigation needs to be done in order to verify exosome uptake.
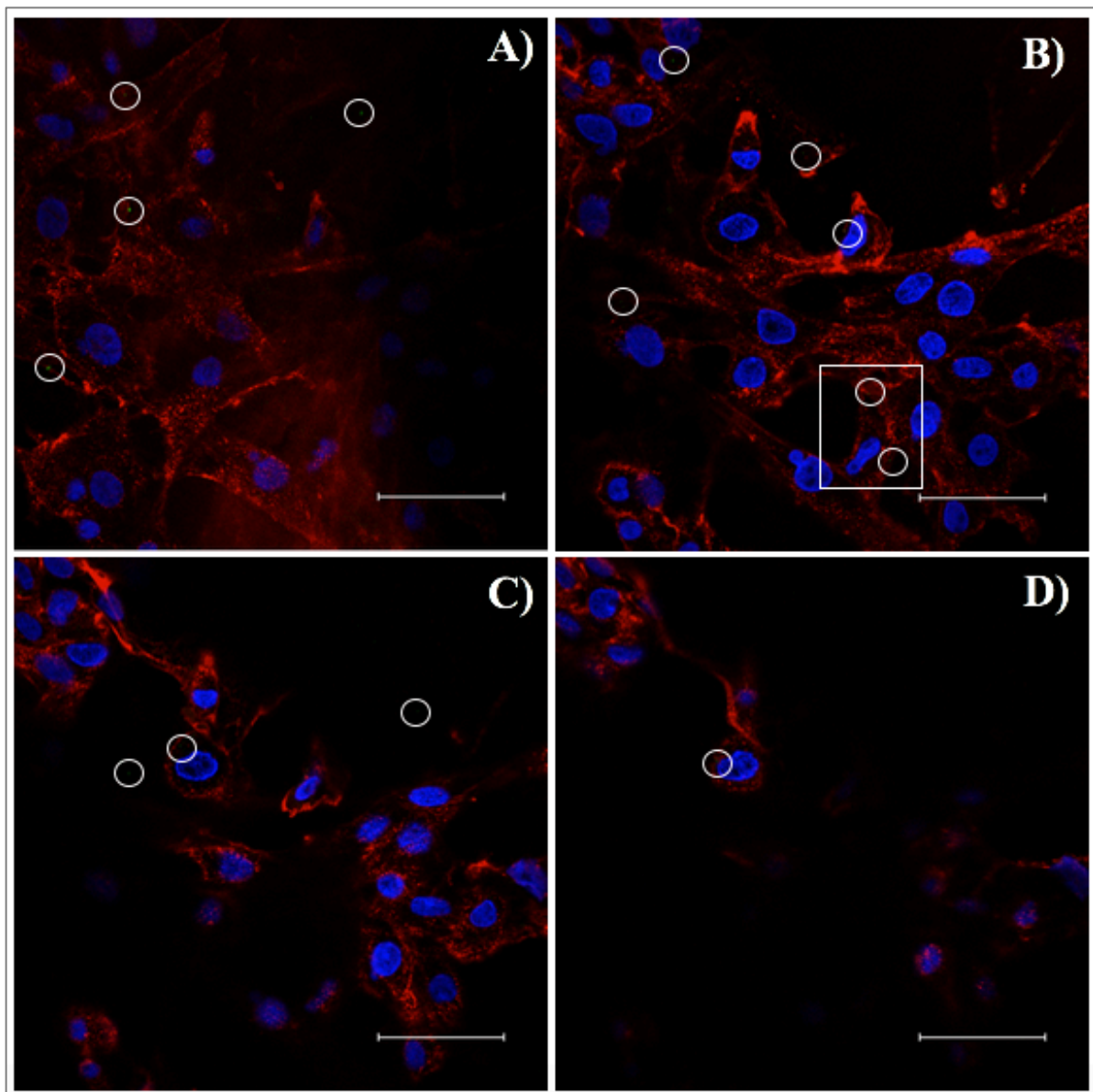
Figure 4.13: Three-dimensional image of the cells by collecting multiple focal planes in a z-stack, 3 μm step. In total 14 exosomes, indicated by circles, were detected. (**A**) Stack 1, presenting the bottom of the cells. Four exosomes were identified in this stack. Bar, 50 μm. (**B**) Stack 2. Exosomes are observed to be inside the cell (indicated by a rectangle). Bar, 50

μm. (**C**) Stack 3. Three exosomes were identified in this stack. Bar, 50 μm. (**D**) Stack 4, presenting the top of the cells. One exosome identified. Bar, 50 μm.

Figure 4.14: Blow up of rectangle from Figure 4.13B. Exosomes (marked with arrows) are only to be found in this stack, indicating that the exosomes may be inside the cell.

5. Discussion

5.1 Evaluation of SEC as an isolation method

A major challenge in utilizing exosomes as a drug delivery system, is the lack of an efficient isolation and purification method. Still there is no efficient method for isolation of exosomes from biological fluids, like plasma, without impurities [39]. Each protocol needs to be optimized depending on the source of biological sample in 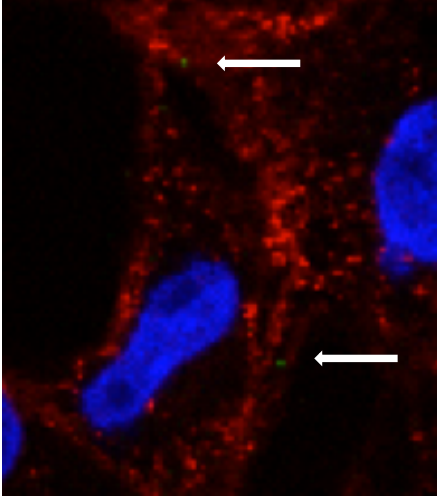order to achieve a high yield of exosomes without impurities, and often several methods are combined. Isolation of plasma derived exosomes is difficult due to the high viscosity of blood and the presence of many proteins and lipoproteins, including fibrinogen and albumin [36, 37]. In addition they are derived from many different cell types, like endothelial cells, leukocytes, platelets and red cells, which again complicates their analysis [38]. However, studies show that EVs in blood plasma are very stable and are considered a possible nanocarrier for drug delivery systems [66].

In this study size exclusion chromatography (SEC) was tested and optimized to isolate blood plasma derived exosomes. This method was selected as it is proven to isolate without impurities, and it maintains the vesicular structure and conformation of the exosomes. Although the manual collection of fractions was expected to introduce some variability, the size of the different fractions was observed to be similar in all isolations. Exosomes with high homogeneity were found to predominantly elute in fraction 10 and 11. Fraction 7, 8 and 9 were concluded to not be exosome fractions and were excluded from further studies.

The next step was to assess the sample quality by analyzing the protein content of the exosome fractions. This revealed high protein content in most of the fractions, especially around 62 kDa, indicating high amount of albumin in the samples. Furthermore, immunoglobulin and fibrinogen beta were identified as highly abundant proteins in the MS analysis. Although SEC is proposed to be an isolation method without impurities, there is evidence that small proteins may co-purify [40]. These findings strongly suggest that an additional purification step is needed in order to get pure vesicle fractions. Ultrafiltration with a 100K filter device was applied and verified as a possible protein removal method. Other studies are consistent with the findings that ultrafiltration (100K) can be used for EV

purification [67, 68]. Another study reveals that ultrafiltration by a 10K device results in complete EV recovery, whereas recovery for 100K filters was only 40% [69]. Further testing is required to determine which filter device that will obtain the highest yield of pure exosomes. The results in this study strongly suggest that SEC is a possible isolation method for plasma derived exosomes, however the actual yield of exosomes should be analyzed in order to confirm this as a preferable isolation method.

It is difficult to establish SEC as a good method without determining the actual yield of exosomes after isolation. There are a variety of exosome quantification techniques, but this is a relatively new field and currently there is no optimal approach. Current methods are not able to distinguish the exosomes from other EVs, making it difficult to determine the actual concentration of exosomes. SEC is known to have some limitations, such as the manual collection of fractions, that may introduce variability and can affect the purity [41]. Dilution of the samples may also lead to yield loss, as an additional concentrating step often is required. In addition, if one wish to isolate exosomes from a high amount of sample, the processing time would be time consuming as the maximum sample volume of the column is 0.5 mL. Nevertheless, SEC is well confirmed in order to obtain high purity exosomes [36, 67, 70]. However, it is plausible that adjusting sample volume, type of medium or optimizing the applied sample prior to application might improve exosome yields in the SEC method [39, 65]. Immunoaffinity capture is a method that isolates exosomes with high purity, but at the same time lower yields are obtained [25]. Still, this would be an ideal method to apply in addition to SEC, in order to achieve more purified exosomes in the analysis. A standardized isolation method resulting in pure exosomes still needs to be defined to provide the opportunity for further research of the proteomic, lipidomics and structural biology of exosomes.

5.2 Size distribution and poly-dispersity of fractions

The particle size distribution and PDI values of exosomes are highly important characteristics that needs to be assessed in order to be considered as nanocarriers. To achieve optimum clinical outcomes by using exosomes as nanocarriers, a constant and narrow size distribution is necessary. Furthermore, size distribution and particle size are important factors when evaluating the stability of drug loaded exosomes upon storage. The tendency of phospholipid vesicles to accumulate in target tissue depends on their characteristics including particle size

distribution [71]. A homogenous population of exosomes of a certain size is needed in order to achieve a safe, efficient and stable drug transfer.

DLS was applied in this study as a size characterization method. Size distribution of the EVs fractions was determined, and the results indicated that fraction 10, 11 and 12 were exosome fractions. Size distribution gives a good description of the size, however z-average and average poly-dispersity (PDI) gives more reliable results for comparative purposes. As the PDI is below 0.5 the z-average mean is more reliable compared to peak position in distribution analysis [72]. Therefore, the z-average diameter and PDI values, with respect to the size distribution, were considered when determining the size of the isolated fractions. Fraction 10 and 11 were measured to have a z-average ranging from 50-100 nm and were considered as exosome fractions with high particle homogeneity. Where the average PDI was measured to be 0.209±0.010 and 0.212±0.005, respectively. In drug delivery application using phospholipid vesicles, such as exosomes, a PDI of 0.3 and below is considered acceptable and indicates a homogenous population [72].

Size determination by DLS has several advantages compared to other methods. DLS is a highly sensitive, noninvasive method that requires little sample volume. Experiments can also be conducted with a wide range of temperatures as well as different sample buffers. In addition, it can be applied to detect aggregation of proteins in vesicle fractions. The method still suffers from some minor limitations, including the need of a transparent sample and the difficulty in separation of closely related molecules. Moreover, DLS is primarily based on the Brownian motion of particles in a solution which is size, temperature and solvent viscosity dependent. Therefore, accurate temperature is essential in order to get a reliable DLS measurement [48]. Even a small amount of large aggregates will affect the measurements, therefore sufficient cleaning of the cuvette and sample filtration must be done prior to DLS experiments. Other common size characterization methods of nanoparticles include NTA and TEM. Where NTA can provide information about the relative concentration of microvesicles, leading to a better standardization of systems. But at the same time, exosomes are difficult to distinguish from other microvesicles by this technique. TEM can determine the morphology of nanoparticles, but the sample require extensive preparation that easily can result in changed morphology of exosomes [43]. Nevertheless, DLS appears to be the preferable method in this analysis, providing information about particle size, homogeneity and aggregation.

5.3 Proper storage condition of exosomes

There is a lack of studies providing information on the effect of storage conditions to exosomes. In order to study and apply exosomes as a drug delivery system, it is important to establish storage conditions that will keep the exosomes stable and intact until use. Long-time storage at -80°C is considered to preserve the exosomes [73, 74]. However, not much is known about short-term storage of exosomes.

The biophysical and protein content of exosomes were observed to change upon storage, therefore, different storage conditions were tested in order to keep the exosomes stable until use. DLS was applied to analyze the size distribution, and lipid and protein content was measured by absorbance. In this experiment multiple freezing and thawing cycles were found to affect the exosomes drastically. Indicating that exosomes need to be aliquoted prior to freezing in order to prevent degradation. However, the ultrafiltrated fraction (9X, 100K) stored at -20°C, showed no signs of degradation after thawing. Indicating that removal of residual proteins aid to keep exosomes stable during multiple freezing and thawing cycles. The best short-term storage condition was observed to be 4°C and 20°C, at these temperatures the size distribution showed little sign of degradation. Furthermore, the lipid and protein content were observed to be constant during the days of storage at these temperatures.

These results, as a part of the larger exosome study, provide information about preservation of exosomes and will aid in future application studies. However, it would be favorable to study several fractions over a longer period of time in order to compare and determine the best storage condition. Previous studies report reduced biological activity of stored exosomes when compared to fresh isolates, suggesting comprised ability to transfer cargo into recipient cell [75]. Therefore, the biological activity of the exosomes after storage should be assessed in order to confirm their ability to transfer cargo. As exosomes and their contents are susceptible to degradation, they should be applied directly after isolation to avoid the risk of degradation by storage.

5.4 Proteomic analysis of exosomes

Despite the increased interest of exosomes, complex biological fluids like plasma, still pose a significant challenge in the proteomic analysis of exosomes. Exosomes contain many specific

proteins and lipids that can be utilized in characterization. Nevertheless, exosomal proteins are difficult to identify as they are low abundant proteins in the vesicle fractions. Due to the rapid improvements in proteomic methods, characterization by exosomal protein is achievable and continuing to expand.

Mass spectrometry is a method that can be applied to get qualitative and quantitative information on the molecular composition of exosomes [54]. The quality of the mass spectra is dependent on sample purity and amount of sample. In this experiment, no exosomal proteins were detected in the isolated fractions by MS. However, immunoglobulin and fibrinogen beta were identified as highly abundant proteins. The main challenges in a MS based proteomic analysis of plasma derived exosomes, include the sample preparation method and potential contamination from plasma. Proper sample preparation is especially critical when detecting low abundance components of a sample, as abundant contaminants may block the detection. In addition, the concentration of exosomal proteins was expected to be low and hence difficult to detect by CBB. An alternative method would be to run the sample in SDS-PAGE for a shorter period of time to prevent protein separation, and consequently be able to process the whole sample by in-gel digestion [76].

Tetraspanin proteins are exosome-associated surface markers resulting from exosome formation in MVBs, and are commonly used to identify proteins in western blotting [23]. WB is a highly sensitive and specific method, hence able to detect low abundant proteins by immunoprecipitation by the use of a specific antibody [77]. The WB results showed high expression of tetraspanin CD9 in the predicted height (28 kDa) on sample F13, indicating that exosomal proteins are present in this vesicle fraction. This would suggest that WB is a more sensitive method, compared to MS, when identifying low abundance proteins in a complex mixture. However, CD9 was only identified in one fraction, and further investigation is needed in order to identify the exosomal protein in all of the exosome fractions. Although western blotting is the most commonly used method for protein identification, the method is reported to have challenges that can cause inconsistent results [77]. One limitation is that the transfer efficiency can be affected by varying gel concentrations, leading to loss of proteins during transfer [77]. Other problems include rapid degradation of detection signal, high background or that the antibody can interaction with other proteins leading to incorrect interpretation [78]. In order to achieve reliable results in WB, antibodies should be validated by both positive and negative controls to ensure specificity [78]. The CD9 detection in this

experiment would have been more reliable if controls were applied to verify the protein identification.

Characterization by MS can provide both qualitative and quantitative information about protein and lipids of exosomes, and this would be the preferable characterization method if the sample contained pure exosomes. On the other hand, WB allows for detection of low abundant proteins in complex samples. Therefore, this was considered as the best characterization method in this study. Several controls should have been applied in order to verify the detection of CD9.

5.5 Exosome uptake by astrocytes

To investigate exosomes as a drug delivery system in neurological diseases, one of the most important criteria to be considered is the cellular uptake. This confirms that exosomes are able to cross the BBB and deliver their cargo. The exosome uptake mechanism by a recipient cell is cell-specific and still not unraveled. Therefore, it is important to establish exosome uptake by the BBB cells to confirm that drugs can be transported into the brain.

Rat astrocytes were incubated with exosomes for 20 minutes, followed by visualization by a confocal microscope to investigate the BBB permeability of endogenous exosomes. Exosomes were detected in around 80% of the scans, this validates that exosomes were successfully stained by the pellet method. Several single confocal scans were captured showing exosomes close to the cells. But verification that exosomes actually are inside the cells was difficult with this type of image. Therefore, further investigation was done by capturing multiple focal planes in a z-stack to get a better understanding in the exosome uptake by astrocytes. The three-dimensional image reveled that two exosomes were present inside the astrocytes. Although this may be indication of exosome uptake by the cells, further investigation needs to be done in order to verify exosome uptake. Varying incubation time with exosomes and different concentrations of exosomes are some aspects that should be included in future investigation.

For exosomes to be considered to *in vivo* application in refractory epilepsy, cellular uptake is one of the most important criteria to establish. Researchers have successfully delivered siRNA into a mouse brain by exosomes without non-specific uptake in other tissues [79]. The

exosomes were intravenously injected proving that exosome cargo can be delivered into the brain, demonstrating the therapeutic potential in exosome delivery. Another recent study demonstrated the capacity of brain endothelial cell derived exosomes to deliver cancer drugs across the BBB in a zebra fish model [27]. Exosomes carry cell-type-specific proteins inherited from their parent cell, and neural derived exosomes are thought to provide a better transport over the BBB compared to other cell derived exosomes [27]. Plasma derived exosomes are derived from, amongst others, endothelial cells. This may contribute to a better exosome transport across the BBB. Confocal microscopy and other methods, like flow cytometry [80] or MS, should be applied in the exosome uptake study to find the most efficient and reliable method. The fact that endothelial cells and astrocytes release their own exosomes may complicate the analysis, but neural secreted exosomes carry specific proteins that can be utilized to distinguish neural exosomes from applied exosomes [32].

6. Conclusion and future perspectives

This study has established that endogenous exosome isolation from plasma is possible by SEC, where exosomes are predominantly eluting in fraction 10, 11 and 12. Furthermore, ultrafiltration (100K) was introduced and showed great promise as a purification method of vesicle fractions. Z-average and PDI was analyzed to determine vesicle size and homogeneity, and fraction 10 and 11 were confirmed to have high particle homogeneity. Short-term storage of exosomes was tested, and 4°C and 20°C was confirmed as the best temperatures in order to preserve the exosomes. Confocal results suggest that exosomes are taken up by rat astrocytes, this indicates that exosomes are able to cross the BBB and deliver their cargo.

In order to explore exosomes potential as nanocarriers in neurological diseases, like refractory epilepsy, many problems require further investigation. It is crucial to know the specific functions of exosomes, and their biological roles in the CNS. The role of exosomes in health and disease is not fully understood making it complicated to predict a long-term safety and therapeutic effect. Exosomes involvement in tumor growth and enhanced tumor cell survival is also a huge concern [28]. Before exosomes can be used as a drug delivery system, future investigation is needed to fully understand the biology of exosomes. Like the immune reactions, circulation and accumulation of exosomes in the human body. Successful loading of AEDs into exosomes must be confirmed, as well as study of the cargo delivery to target cell. A standardized isolation method resulting in pure vesicle fractions, as well as a proper characterization method, need to be established for better advancement of ongoing exosome research. Future investigation should reveal exosome uptake by BBB cells to confirm that AEDs can be transferred into the brain. This is still a new field and the best methods are yet to be described.

References

1.   Ballabh, P., A. Braun, and M. Nedergaard, *The blood-brain barrier: an overview: structure, regulation, and clinical implications.* Neurobiol Dis, 2004. **16**(1): p. 1-13.
2.   van Vliet, E.A., et al., *Blood-brain barrier leakage may lead to progression of temporal lobe epilepsy.* Brain, 2007. **130**(Pt 2): p. 521-34.
3.   Daneman, R. and A. Prat, *The blood-brain barrier.* Cold Spring Harb Perspect Biol, 2015. **7**(1): p. a020412.
4.   Liu, W.Y., et al., *Tight junction in blood-brain barrier: an overview of structure, regulation, and regulator substances.* CNS Neurosci Ther, 2012. **18**(8): p. 609-15.
5.   Hartsock, A. and W.J. Nelson, *Adherens and tight junctions: structure, function and connections to the actin cytoskeleton.* Biochim Biophys Acta, 2008. **1778**(3): p. 660-9.
6.   Meng, W. and M. Takeichi, *Adherens junction: molecular architecture and regulation.* Cold Spring Harb Perspect Biol, 2009. **1**(6): p. a002899.
7.   Bazzoni, G. and E. Dejana, *Endothelial cell-to-cell junctions: molecular organization and role in vascular homeostasis.* Physiol Rev, 2004. **84**(3): p. 869-901.
8.   Reese, T.S. and M.J. Karnovsky, *Fine structural localization of a blood-brain barrier to exogenous peroxidase.* J Cell Biol, 1967. **34**(1): p. 207-17.
9.   Banks, W.A., *Characteristics of compounds that cross the blood-brain barrier.* BMC Neurol, 2009. **9 Suppl 1**: p. S3.
10.   Misra, A., et al., *Drug delivery to the central nervous system: a review.* J Pharm Pharm Sci, 2003. **6**(2): p. 252-73.
11.   Dong, X., *Current Strategies for Brain Drug Delivery.* Theranostics, 2018. **8**(6): p. 1481-1493.
12.   Lu, C.T., et al., *Current approaches to enhance CNS delivery of drugs across the brain barriers.* Int J Nanomedicine, 2014. **9**: p. 2241-57.
13.   Jerome Engel, J., *Seizures and epilepsy*. 2013: Oxford University Press.
14.   Kiriakopoulos, E., *www.epilepsy.com, Types of Seizures.* 2017.
15.   Marchi, N., et al., *Blood-brain barrier dysfunction and epilepsy: pathophysiologic role and therapeutic approaches.* Epilepsia, 2012. **53**(11): p. 1877-86.
16.   Marchi, N., et al., *Seizure-promoting effect of blood-brain barrier disruption.* Epilepsia, 2007. **48**(4): p. 732-42.
17.   Pandey, P.K., A.K. Sharma, and U. Gupta, *Blood brain barrier: An overview on strategies in drug delivery, realistic in vitro modeling and in vivo live tracking.* Tissue Barriers, 2016. **4**(1): p. e1129476.
18.   Rogawski, M.A. and W. Loscher, *The neurobiology of antiepileptic drugs.* Nat Rev Neurosci, 2004. **5**(7): p. 553-64.
19.   Oby, E. and D. Janigro, *The blood-brain barrier and epilepsy.* Epilepsia, 2006. **47**(11): p. 1761-74.
20.   French, J.A., *Refractory epilepsy: clinical overview.* Epilepsia, 2007. **48 Suppl 1**: p. 3-7.
21.   Barile, L. and G. Vassalli, *Exosomes: Therapy delivery tools and biomarkers of diseases.* Pharmacol Ther, 2017. **174**: p. 63-78.
22.   Kooijmans, S.A., et al., *Exosome mimetics: a novel class of drug delivery systems.* Int J Nanomedicine, 2012. **7**: p. 1525-41.

23.   Aryani, A. and B. Denecke, *Exosomes as a Nanodelivery System: a Key to the Future of Neuromedicine?* Mol Neurobiol, 2016. **53**(2): p. 818-34.

24.   Fevrier, B. and G. Raposo, *Exosomes: endosomal-derived vesicles shipping extracellular messages.* Curr Opin Cell Biol, 2004. **16**(4): p. 415-21.

25.   Li, P., et al., *Progress in Exosome Isolation Techniques.* Theranostics, 2017. **7**(3): p. 789-804.

26.   Raposo, G. and W. Stoorvogel, *Extracellular vesicles: exosomes, microvesicles, and friends.* J Cell Biol, 2013. **200**(4): p. 373-83.

27.   Yang, T., et al., *Exosome delivered anticancer drugs across the blood-brain barrier for brain cancer therapy in Danio rerio.* Pharm Res, 2015. **32**(6): p. 2003-14.

28.   Ha, D., N. Yang, and V. Nadithe, *Exosomes as therapeutic drug carriers and delivery vehicles across biological membranes: current perspectives and future challenges.* Acta Pharm Sin B, 2016. **6**(4): p. 287-96.

29.   Lai, C.P. and X.O. Breakefield, *Role of exosomes/microvesicles in the nervous system and use in emerging therapies.* Front Physiol, 2012. **3**: p. 228.

30.   Willis, C.M., et al., *A Refined Bead-Free Method to Identify Astrocytic Exosomes in Primary Glial Cultures and Blood Plasma.* Front Neurosci, 2017. **11**: p. 335.

31.   Verkhratsky, A., et al., *Astrocytes as secretory cells of the central nervous system: idiosyncrasies of vesicular secretion.* EMBO J, 2016. **35**(3): p. 239-57.

32.   Kanninen, K.M., et al., *Exosomes as new diagnostic tools in CNS diseases.* Biochim Biophys Acta, 2016. **1862**(3): p. 403-10.

33.   Pan, B.T. and R.M. Johnstone, *Fate of the transferrin receptor during maturation of sheep reticulocytes in vitro: selective externalization of the receptor.* Cell, 1983. **33**(3): p. 967-78.

34.   van Niel, G., et al., *Exosomes: a common pathway for a specialized function.* J Biochem, 2006. **140**(1): p. 13-21.

35.   Lakkaraju, A. and E. Rodriguez-Boulan, *Itinerant exosomes: emerging roles in cell and tissue polarity.* Trends Cell Biol, 2008. **18**(5): p. 199-209.

36.   Boing, A.N., et al., *Single-step isolation of extracellular vesicles by size-exclusion chromatography.* J Extracell Vesicles, 2014. **3**.

37.   van der Pol, E., et al., *Optical and non-optical methods for detection and characterization of microparticles and exosomes.* J Thromb Haemost, 2010. **8**(12): p. 2596-607.

38.   Dragovic, R.A., et al., *Sizing and phenotyping of cellular vesicles using Nanoparticle Tracking Analysis.* Nanomedicine, 2011. **7**(6): p. 780-8.

39.   Baranyai, T., et al., *Isolation of Exosomes from Blood Plasma: Qualitative and Quantitative Comparison of Ultracentrifugation and Size Exclusion Chromatography Methods.* PLoS One, 2015. **10**(12): p. e0145686.

40.   Taylor, D.D. and S. Shah, *Methods of isolating extracellular vesicles impact down-stream analyses of their cargoes.* Methods, 2015. **87**: p. 3-10.

41.   Stranska, R., et al., *Comparison of membrane affinity-based method with size-exclusion chromatography for isolation of exosome-like vesicles from human plasma.* J Transl Med, 2018. **16**(1): p. 1.

42.   Contreras-Naranjo, J.C., H.J. Wu, and V.M. Ugaz, *Microfluidics for exosome isolation and analysis: enabling liquid biopsy for personalized medicine.* Lab Chip, 2017. **17**(21): p. 3558-3577.

43. Szatanek, R., et al., *The Methods of Choice for Extracellular Vesicles (EVs) Characterization.* Int J Mol Sci, 2017. **18**(6).

44. Yanez-Mo, M., et al., *Biological properties of extracellular vesicles and their physiological functions.* J Extracell Vesicles, 2015. **4**: p. 27066.

45. Soo, C.Y., et al., *Nanoparticle tracking analysis monitors microvesicle and exosome secretion from immune cells.* Immunology, 2012. **136**(2): p. 192-7.

46. Akers, J.C., et al., *Comparative Analysis of Technologies for Quantifying Extracellular Vesicles (EVs) in Clinical Cerebrospinal Fluids (CSF).* PLoS One, 2016. **11**(2): p. e0149866.

47. Witwer, K.W., et al., *Standardization of sample collection, isolation and analysis methods in extracellular vesicle research.* J Extracell Vesicles, 2013. **2**.

48. Stetefeld, J., S.A. McKenna, and T.R. Patel, *Dynamic light scattering: a practical guide and applications in biomedical sciences.* Biophys Rev, 2016. **8**(4): p. 409-427.

49. Millipore, *User Guide Amicon Ultra-0.5 Centrifugal Filter Devices.* 2011.

50. ThermoScientific, *Instructions Pierce BCA Protein Assay Kit.* 2013.

51. ThermoScientific, *Bolt Mini Gels User Manual.* 2014.

52. Weksler, B., I.A. Romero, and P.O. Couraud, *The hCMEC/D3 cell line as a model of the human blood brain barrier.* Fluids Barriers CNS, 2013. **10**(1): p. 16.

53. EndoGRO Media Products for Human Endothelial Cell Culture, P.M., *Millipore.* 2008.

54. Finehout, E.J. and K.H. Lee, *An introduction to mass spectrometry applications in biological research.* Biochem Mol Biol Educ, 2004. **32**(2): p. 93-100.

55. Granvogl, B., M. Ploscher, and L.A. Eichacker, *Sample preparation by in-gel digestion for mass spectrometry-based proteomics.* Anal Bioanal Chem, 2007. **389**(4): p. 991-1002.

56. ThermoScientific, *Instructions In-Gel Tryptic Digestion Kit.* 2013.

57. Hale, J.E., et al., *A simplified procedure for the reduction and alkylation of cysteine residues in proteins prior to proteolytic digestion and mass spectral analysis.* Anal Biochem, 2004. **333**(1): p. 174-81.

58. ThermoScientific, *Instructions Pierce C18 Spin Columns.* 2011.

59. Smith, M., Y. Omidi, and M. Gumbleton, *Primary porcine brain microvascular endothelial cells: biochemical and functional characterisation as a model for drug transport and targeting.* J Drug Target, 2007. **15**(4): p. 253-68.

60. Thomsen, L.B., A. Burkhart, and T. Moos, *A Triple Culture Model of the Blood-Brain Barrier Using Porcine Brain Endothelial cells, Astrocytes and Pericytes.* PLoS One, 2015. **10**(8): p. e0134765.

61. Sofroniew, M.V. and H.V. Vinters, *Astrocytes: biology and pathology.* Acta Neuropathol, 2010. **119**(1): p. 7-35.

62. Deli, M.A., et al., *Permeability studies on in vitro blood-brain barrier models: physiology, pathology, and pharmacology.* Cell Mol Neurobiol, 2005. **25**(1): p. 59-127.

63. Pawley, J.B., *Handbook of biological confocal microscopy.* 3rd ed. 2006, New York: Springer. xxviii, 985 p.

64. Combs, C.A., *Fluorescence microscopy: a concise guide to current imaging methods.* Curr Protoc Neurosci, 2010. **Chapter 2**: p. Unit2 1.

65. Izon, *qEVoriginal Size Exclusion Column, Specifications and Operational Guide.*

66. Kalra, H., et al., *Comparative proteomics evaluation of plasma exosome isolation techniques and assessment of the stability of exosomes in normal human blood plasma.* Proteomics, 2013. **13**(22): p. 3354-64.

67.   Nordin, J.Z., et al., *Ultrafiltration with size-exclusion liquid chromatography for high yield isolation of extracellular vesicles preserving intact biophysical and functional properties.* Nanomedicine, 2015. **11**(4): p. 879-83.

68.   Mol, E.A., et al., *Higher functionality of extracellular vesicles isolated using size-exclusion chromatography compared to ultracentrifugation.* Nanomedicine, 2017. **13**(6): p. 2061-2065.

69.   Benedikter, B.J., et al., *Ultrafiltration combined with size exclusion chromatography efficiently isolates extracellular vesicles from cell culture media for compositional and functional studies.* Sci Rep, 2017. **7**(1): p. 15297.

70.   Welton, J.L., et al., *Ready-made chromatography columns for extracellular vesicle isolation from plasma.* J Extracell Vesicles, 2015. **4**: p. 27269.

71.   Danaei, M., et al., *Impact of Particle Size and Polydispersity Index on the Clinical Applications of Lipidic Nanocarrier Systems.* Pharmaceutics, 2018. **10**(2).

72.   Malvern, *Zetasizer nano user manual.* 2013.

73.   Cheng, Y., et al., *Effect of pH, temperature and freezing-thawing on quantity changes and cellular uptake of exosomes.* Protein Cell, 2019. **10**(4): p. 295-299.

74.   Lee, M.I., W.; Kim,M.; Ban, J.J., *Influence of storage condition on exosome recovery.* 2016.

75.   Sterzenbach, U., et al., *Engineered Exosomes as Vehicles for Biologically Active Proteins.* Mol Ther, 2017. **25**(6): p. 1269-1278.

76.   Wang, Z., et al., *Proteomic analysis of urine exosomes by multidimensional protein identification technology (MudPIT).* Proteomics, 2012. **12**(2): p. 329-38.

77.   Ghosh, R., J.E. Gilda, and A.V. Gomes, *The necessity of and strategies for improving confidence in the accuracy of western blots.* Expert Rev Proteomics, 2014. **11**(5): p. 549-60.

78.   Bass, J.J., et al., *An overview of technical considerations for Western blotting applications to physiological research.* Scand J Med Sci Sports, 2017. **27**(1): p. 4-25.

79.   Alvarez-Erviti, L., et al., *Delivery of siRNA to the mouse brain by systemic injection of targeted exosomes.* Nat Biotechnol, 2011. **29**(4): p. 341-5.

80.   Czernek, L., A. Chworos, and M. Duechler, *The Uptake of Extracellular Vesicles is Affected by the Differentiation Status of Myeloid Cells.* Scand J Immunol, 2015. **82**(6): p. 506-14.

APPENDIX

Z-average diameter and PDI values retrieved from the Zetasizer software.

Table 1: Z-average diameter and PDI values of fraction stored in room temperature (F11). SD was calculated.

Day	Average size (Z-Average, d.nm)	Average PDI
0	$53,210 \pm 0,318$	$0,177 \pm 0,011$
1	$54,557 \pm 0,146$	$0,195 \pm 0,006$
2	$56,493 \pm 0,342$	$0,216 \pm 0,004$
3	$59,770 \pm 0,165$	$0,255 \pm 0,004$
8	$88,213 \pm 0,522$	$0,278 \pm 0,006$

Table 2: Z-average diameter and PDI values of fraction stored in 4°C (F11). SD was calculated.

Day	Average size (Z-Average, d.nm)	Average PDI
0	$53,210 \pm 0,318$	$0,177 \pm 0,011$
1	$53,896 \pm 0,151$	$0,190 \pm 0,012$
2	$55,420 \pm 0,241$	$0,213 \pm 0,004$
3	$54,597 \pm 0,351$	$0,187 \pm 0,006$
8	$55,887 \pm 0,118$	$0,210 \pm 0,003$

Table 3: Z-average diameter and PDI values of fraction stored in -20°C (F11). SD was calculated

Day	Average size (Z-Average, d.nm)	Average PDI
0	$53,210 \pm 0,318$	$0,177 \pm 0,011$
1	$114,666 \pm 3,583$	$0,346 \pm 0,081$
2	$154,566 \pm 0,601$	$0,464 \pm 0,063$
3	$249,000 \pm 36,222$	$0,672 \pm 0,097$
8	$314,300 \pm 104,471$	$0,761 \pm 0,005$

Table 4: Z-average diameter and PDI values of fraction stored in -80°C (F11). SD was calculated

Day	Average size (Z-Average, d.nm)	Average PDI
0	53,210 ± 0,318	0,177 ± 0,011
1	91,377 ± 1,097	0,263 ± 0,008
2	141,100 ± 2,736	0,385 ± 0,005
3	195,300 ± 3,758	0,469 ± 0,070
8	349,300 ± 78,954	0,708 ± 0,013

Table 5: Z-average diameter and PDI values of fraction applied in the confocal microscopy analysis. SD was calculated.

Fraction	Average size (Z-Average, d.nm)	Average PDI
12	50,187 ± 0,245	0,209 ± 0,004